

AD-A137 122      LONGITUDINAL RESISTIVITY AND INTERMEDIATE MACH NUMBER  
COLLISIONLESS TRANSVERSE MAGNETOSONIC SHOCKS(U) NAVAL  
RESEARCH LAB WASHINGTON DC W M MANHEIMER ET AL.

1/1

UNCLASSIFIED

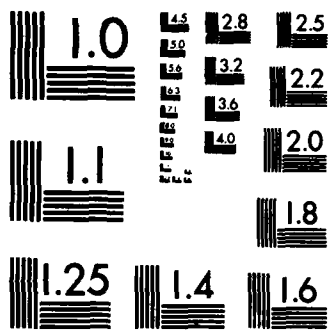
30 DEC 83 NRL-MR-5243

F/G 20/4

NL

END:

FORMED  
FBI  
DHC



MICROCOPY RESOLUTION TEST CHART  
NATIONAL BUREAU OF STANDARDS-1963-A

# **NRL Memorandum Report 5243**

AD A 1 3 7 1 2 2

# **Longitudinal Resistivity and Intermediate Mach Number Collisionless Transverse Magnetosonic Shocks**

W. M. MANHEIMER AND D. S. SPICER\*

*Plasma Theory Branch  
Plasma Physics Division*

**\*Geophysical and Plasma Dynamics Branch  
Plasma Physics Division**

**December 30, 1983**

**This research was sponsored by the Defense Nuclear Agency under Subtask S99QMXBC, work unit 00094 and work unit title "Burst Structure Sources."**



**NAVAL RESEARCH LABORATORY**  
**Washington, D.C.**

10123 1694

Approved for public release; distribution unlimited.

# TC FILE COPY

REPORT DOCUMENTATION PAGE		READ INSTRUCTIONS BEFORE COMPLETING FORM
1. REPORT NUMBER NRL Memorandum Report 5243	2. GOVT ACCESSION NO. <i>AD-A137 122</i>	3. RECIPIENT'S CATALOG NUMBER
4. TITLE (and Subtitle) LONGITUDINAL RESISTIVITY AND INTERMEDIATE MACH NUMBER COLLISIONLESS TRANSVERSE MAGNETOSONIC SHOCKS	5. TYPE OF REPORT & PERIOD COVERED Interim report on a continuing NRL problem.	
7. AUTHOR(s) W.M. Manheimer and D.S. Spicer	6. PERFORMING ORG. REPORT NUMBER	
9. PERFORMING ORGANIZATION NAME AND ADDRESS Naval Research Laboratory Washington, DC 20375	10. PROGRAM ELEMENT, PROJECT, TASK AREA & WORK UNIT NUMBERS 62715H; 47-1944-0-3	
11. CONTROLLING OFFICE NAME AND ADDRESS Defense Nuclear Agency Washington, DC 20305	12. REPORT DATE December 30, 1983	
14. MONITORING AGENCY NAME & ADDRESS (if different from Controlling Office)	13. NUMBER OF PAGES 60	
16. DISTRIBUTION STATEMENT (of this Report)	15. SECURITY CLASS. (of this report) UNCLASSIFIED	
17. DISTRIBUTION STATEMENT (of the abstract entered in Block 20, if different from Report)	18e. DECLASSIFICATION/DOWNGRADING SCHEDULE	
18. SUPPLEMENTARY NOTES This research was sponsored by the Defense Nuclear Agency under Subtask S99QMXBC, work unit 00094 and work unit title "Burst Structure Sources."	19. KEY WORDS (Continue on reverse side if necessary and identify by block number) Collisionless shocks                    Magnetosonic shocks Supercritical shocks                    Ion reflection	
20. ABSTRACT (Continue on reverse side if necessary and identify by block number) It is shown that for collisionless transverse magnetosonic shocks, there exists an intermediate range of Mach numbers between the maximum Mach number for transverse resistivity and the onset of significant ion reflection. In this intermediate range, the structure is dominated by a breakdown of the quasi-neutrality approximation and longitudinal resistivity is a simple fluid model for the dissipation mechanism which forms the shock.		

## CONTENTS

I.	Introduction.....	1
II.	Review of the Results of Laboratory Experiments on Transverse Collisionless Shocks.....	6
III.	Shocks with Transverse and Longitudinal Resistivity.....	10
	A. Review of Shocks Formed by Transverse Resistivity.....	11
	B. Shocks with Longitudinal Resistivity.....	17
	C. Calculating the Double Structured Shock.....	23
IV.	Nonlocal Dissipation and Estimates for $v_\ell$ and $\alpha_\ell$ ..	26
V.	Results.....	33
	A. The Case of Strong Ion Heating.....	33
	B. Shocks with No Ion Heating.....	35
VI.	Conclusions.....	37
	Acknowledgment.....	37
	Appendix A.....	43
	Appendix B.....	45
	References.....	48

Accession For  
NTIS GRAV  
FILE TAB  
1



# LONGITUDINAL RESISTIVITY AND INTERMEDIATE MACH NUMBER COLLISIONLESS TRANSVERSE MAGNETOSONIC SHOCKS

## I. Introduction

It is now reasonably well established that transverse collisionless shocks can exist in at least two Mach number regimes. For  $m$  (the magnetosonic Mach number) less than about 2.5, transverse resistivity is the dissipation mechanism which forms the shock.<sup>1-5</sup> Since the plasma is nearly collisionless, this resistivity is anomalous in that it is assumed to arise from an electron-ion streaming instability in the shock front. Measurements of the turbulent spectrum in the shock front show that fluctuations with wavenumber  $k \sim k_D$ , the Debye wavenumber, are indeed excited.<sup>3,6</sup> It is generally assumed that the resistive dissipation heats only the electrons. However a small amount of ion heating cannot be ruled out. It is certainly not easy to see how an instability can heat only one species. An ion acoustic instability, at least, does give rise to a small amount of ion heating.<sup>7</sup> In fact one theory of the resistive shock structure<sup>8</sup> has this small ion heating playing an important role in determining shock structure.

For larger  $m$ , it is now well established both from theory<sup>9,10,11</sup> and particle simulations,<sup>12-19</sup> that ion reflection from the shock front can act as a dissipation mechanism in one of two ways. On the one hand, these reflected ions may stream ahead of the shock if they are unmagnetized or sufficiently weakly magnetized.<sup>9,10,12-15</sup> If this be the case, the standard Rankine-Hugoniot conservation relations do not apply because of the additional species upstream. On the other hand, the reflected ions may turn around in the magnetic field and drift downstream, their large Larmor orbit velocity effectively becoming part of the downstream pressure.<sup>11,16-19</sup> Since there is no additional upstream species in this

Manuscript approved October 27, 1983.

case, Rankine-Hugoniot conservation relations do apply. In fact the simulations of Refs. 18-19 were successful because the Rankine-Hugoniot relations were exploited in initializing the system. Of course for the latter dissipation mechanism to be significant, the time of the experiment or simulation must be longer than about  $\pi/\omega_{ci}$ , where  $\omega_{ci}$  is the ion cyclotron frequency.

The purpose of this paper is to show that between these two ranges of Mach number, there exists an intermediate range. In this intermediate range, the shock structure and dissipation are dominated by the breakdown of the quasi-neutral approximation. Above a critical Mach number, the quasi-neutral fluid equations predict infinite slope, implying, of course, the breakdown of quasi-neutrality. However, the full set of fluid equations, including charge separation, are nonsingular. Thus, above this Mach number, the flow sets up an electrostatic ion acoustic wave train. The Landau damping of this wave is the dissipation mechanism which forms the shock. This Landau damping may heat either the electrons or ions. In purely electrostatic shocks with very cold ions, the electron Landau damping seems to dominate.<sup>20</sup> Since the electron Landau damping rate is small, the shock structure is oscillatory. On the other hand, in magnetosonic shocks the ions are warmer, so ion Landau damping dominates and the shock structure is monotonic. It is interesting that this dissipation mechanism does not rely on exciting some plasma instability in the shock front, and in that sense it is not anomalous. Indeed, the electrostatic subshock has a Debye length scale size, so it is almost impossible that an instability with still smaller wavelength could be excited.

While this dissipation mechanism is not anomalous it is very complicated. The simplest model of it shows that it is nonlocal, and in that sense non fluid like. However, there is a new simple fluid dissipation model. When the electrostatic oscillation is set up, the longitudinal electron and ion velocities are no longer equal. A longitudinal friction force between the two is an additional possible dissipation mechanism which apparently has not been examined in the previous literature on high Mach shock waves. An important purpose of this paper is to investigate the effect of such longitudinal resistivity on shock structures. Our conclusion is that it is a very good fluid model for collisionless magnetosonic shocks with Mach number in the intermediate regime. It has a precise onset, namely when the shock reaches the critical Mach number. It shows that shocks above this Mach number have an electrostatic subshock embedded within in and its structure is governed by longitudinal resistivity. When the Mach number increases to a second critical value, the full fluid equations become singular, and this defines the upper limit of the intermediate range. The interpretation of this second singularity is simply made in terms of ion reflection. Above this point, the shock, if it exists, is governed by ion reflection as described in, for instance, Refs. 9-19. At no point is it either necessary or physically correct to postulate a viscosity.

While the theory we deal with here concerns only steady state shocks, the general conclusions should also apply to non-steady flow of interpenetrating plasmas. Specifically, electrostatic interactions should be important in a recent series of laboratory experiments on the flow of a laser produced plasma through a background magnetized plasma.<sup>21</sup>

In Section II we review experimental data on high Mach shock structures and show that it indicates the existence of this intermediate regime. To do so, we note that in this Mach number range many of the experiments are over in a time of order of or less than  $\pi/\omega_{ci}$ , so convection of reflected ions downstream<sup>1,3,22,23</sup> cannot be the dissipation mechanism of importance. Also, downstream ion temperatures are measured in several experiments and they agree with Rankine-Hugoniot. This means that pure reflection of unmagnetized ions,<sup>3,22</sup> cannot be the dissipation mechanism either.

In Section III we discuss shock structure for unmagnetized ions where the quasi-neutrality assumption is valid and also where it is not. We find that for sufficiently weakly magnetized plasmas, characteristic of the experiments in Refs. 1-6, 22, 23, the electrostatic and magnetic structures essentially decouple, and that the electrostatic subshock must ride on the crest of the magnetic shock structure. This also agrees with experimental results.

In Section IV, and also in Appendix B, we discuss the actual dissipation mechanism (Landau damping) and fluid models for it. As we show, even the simplest approximation to it is quite complex, and does not easily fit into a simple fluid model. However the actual physical model provides important insight on a best guess for longitudinal resistivity and on the partition of resistive heating between electrons and ions. Another interesting phenomena is that Landau damping can only be a valid long time description of the dissipation mechanism if the shock structure fluctuates in time. Thus the shock cannot be time independent but, of course, its average profile can be.

Section V presents the results of shock structure calculations in the intermediate Mach number regime. Also, where possible, comparisons are made with experimental results. Finally, Section VI draws conclusions.

## II. Review of the Results of Laboratory Experiments

### on Transverse Collisionless Shocks

In this Section we review briefly previous experiments of transverse shocks in laboratory plasmas.<sup>1-6,22,23</sup> Our conclusion, based on examination of this data, is that for  $m \leq 2.5$ , the shocks are resistive, as described by authors of these references. However, there is a range  $2.5 \leq m \leq 5$  where steady shocks form which are above the critical Mach number for resistive shocks. However, the process of ion reflection followed by downstream convection by the  $E \times B$  drift cannot be operative either, if only because the duration of the experiment is less than the ion Larmor time. Furthermore, the dissipation mechanism cannot be simple ion reflection of magnetized ions either. For ion reflection in an unmagnetized plasma, the second ion species upstream drastically alters the Rankine-Hugoniot conditions downstream.<sup>10</sup> However, in two of the experiments cited,<sup>3,22</sup> downstream ion temperatures were measured and found to agree well with Rankine-Hugoniot conditions. Thus our conclusion is that there must be some sort of new dissipation mechanism associated with this intermediate range of Mach numbers.

In Ref. 1, Paul et al. launch shocks with Mach numbers 2.5, 3.7 and 6.3. For the first, resistivity forms the shock and gives the electron heating required to satisfy the Rankine-Hugoniot relations. In the case of  $m = 3.7$ , the downstream electron temperature is less than that predicted by Rankine-Hugoniot, implying that the ions are heated. In addition to the normal magnetic structure, there is a very low amplitude magnetic pedestal in front of the shock. This pedestal is generally interpreted to mean a small number of ions are reflected from the shock front and convect the

magnetic field upstream. However in Paul's experiment, the convection of these ions downstream by the  $E \times B$  drift is almost certainly not the mechanism which forms the shock at  $m = 3.7$ . The shock velocity is about  $2.5 \times 10^7$  cm/sec and the shock propagates ahead of the piston a distance of 10-15 cm, implying a time of about 400 nsec. However,  $\pi/\omega_{ci}$  is also about 400 n sec. Thus any reflected ions cannot make it back behind the shock until the shock hits the cylindrical axis. However, shocks are observed for much shorter times. For the measurement at  $M = 6.3$ , the upstream pedestal broadens and increases in amplitude so that it encompasses the entire shock. At this Mach number, reflected ions are almost certainly playing a role.

In another series of experiments, Keilhacker et al.<sup>3</sup> measured the properties of magnetosonic shock waves with Mach numbers between 1.5 and 5. Here ion temperatures behind the shock are measured by collective scattering of laser light at wavelengths less than the Debye length. The measured ion temperatures agree with Rankine-Hugoniot conditions. In this experiment, the total transit time for the shock is about  $1\mu$  sec. Thus the dissipation mechanism cannot be the convection of reflected ions downstream because there is not enough time; neither can it be the pure reflection of unmagnetized ions, because the downstream ion heating corresponds to that predicted by Rankine-Hugoniot.

Segre and Martone<sup>22</sup> have also investigated transverse shocks in the Mach number range  $3.1 < m < 4.25$ . In their experiment, there is no magnetic field pedestal leading the shock, so reflected ions almost certainly play no role. Even if there were reflected ions, the ion period  $\pi/\omega_{ci} \sim 450$  n sec, the propagation time is only about 250 n sec, so no reflected ions could make it back downstream. In Ref. 22 the downstream

electron density and temperature are measured by laser scattering. However magnetic measurements are used to measure  $n(T_e + T_i)$  downstream, so that downstream ion temperatures can be directly inferred. The measured ion temperatures do in fact agree with that predicted by Rankine-Hugoniot.

Another series of shock experiments are those of Eselevich et al.<sup>23</sup>. The shocks are produced in a tube of 8 cm radius in H, He or A. Since the gas can be varied, and the density varies between  $10^{13} \leq n \leq 10^{15} \text{ cm}^{-3}$  and  $100 \text{ G} < B < 2000 \text{ G}$ , there was a very large parameter space studied. Eselevich et al. found that for Mach numbers between 3 and 5, steady shocks form. In this range of Mach numbers, a pedestal in magnetic field might not lead the shock. For instance, Fig. 2a of Eselevich et al. shows a Mach 4 shock in helium with no pedestal, whereas Fig. 4 shows a Mach 4 shock in hydrogen with a small (i.e., less distinct than in Paul's<sup>1</sup> experiment) magnetic foot leading the shock. Thus, reflected ions are not a universal, and probably not a very important, aspect of steady transverse shocks in this intermediate range of Mach numbers. However, Eselevich et al., like Paul et al., did observe that as the Mach number increases (beyond about 5.5 generally in Ref. 23), the magnetic foot does expand out and dominate the entire structure.

The most distinct feature of Eselevich's observations are that in the intermediate range of Mach numbers, an isomagnetic potential jump forms on the crest of the shock wave. The thickness of the potential jump is typically a Debye length. Thus, a key feature in this intermediate range is the breakdown of the assumption of quasi-neutrality. The potential jump across this isomagnetic transition region initially increases with Mach number, but then above some higher Mach number begins to decrease until above a second critical Mach number, typically about 5 or 6, the entire

isomagnetic jump disappears and the shock structure is taken over by the magnetic pedestal. Hence, we feel that a key element in a fluid description of shocks in this intermediate range is the breakdown of quasi-neutrality. Once quasi-neutrality is violated, an additional fluid dissipation mechanism, longitudinal resistivity becomes possible. In the next two sections we examine the consequence of longitudinal resistivity. Although the actual dissipation mechanism is considerably more complicated and non fluid like (see Sec. IV), a longitudinal resistivity model can explain many features of the experimental results. Specifically it hinges on the breakdown of quasi-neutrality; it provides for the proper electron and/or ion heating; it predicts an isomagnetic potential jump on the crest of the shock wave; and it gives the shock structure only in an intermediate range of Mach numbers between the critical Mach number for transverse resistivity and the onset of strong ion reflection. Thus, longitudinal resistivity is probably as good an approximation to the dissipation mechanism that one can obtain within the limits of a conventional fluid description.

### III. Shocks with Transverse and Longitudinal Resistivity

In this Section, we discuss shocks formed by longitudinal resistivity. Before doing so, however, in Section III.A we set the stage by reviewing the structure of shocks with transverse resistivity. Section III.B discusses the effect of longitudinal resistivity, and Section III.C sets out the procedure for calculating the shock structure in weakly magnetized plasmas.

### A. Review of Shocks Formed by Transverse Resistivity

To start we formulate the equation for quasi-neutral transverse resistive shocks. We neglect both transverse and longitudinal electron inertia, and the motion of the ions in the transverse direction. Assuming that the shock propagates in the  $x$  direction, the magnetic field is in the  $z$  direction, and upstream parameters have a zero subscript, then the electron and ion density equation gives the result

$$nV = n_0 V_0, \quad (1)$$

where a velocity or electric field without a direction subscript means a velocity or electric field in the  $x$  direction. Then the electron momentum equation in the  $x$  and  $y$  direction give respectively equations for  $E$  and  $V_{ey}$ . They are

$$E = -\frac{1}{ne} \frac{d}{dx} n T_e - \frac{V_{ey}}{c} B \quad (2)$$

and

$$V_{ey} = -\frac{eV_0}{mv} \left( B_0 - \frac{n_0}{n} B \right), \quad (3)$$

where  $m$  is the electron mass,  $v$  the effective collision frequency, and the resistive force density on the electrons is  $-nmv(V_{ey} - V_{iy}) \equiv -nmv V_{ey}$  since we assume  $V_{ey} = 0$  (unmagnetized ions). Also we have used the fact that  $E_y = E_{yo} = \frac{V_0}{c} B_0$ .

To write out the electron temperature equation we first assume that the electrons have  $\gamma = 5/3$ . Then we must also specify what fraction of the

resistive heating goes into the electrons and what fraction goes into the ions. In terms of the ion  $\gamma$ , the total energy equation for electrons plus ions is

$$\frac{d}{dx} \left( \frac{1}{2} nM V^3 + \frac{5}{2} nV T_e + \frac{\gamma}{\gamma-1} nV T_i \right) = - n e V_{ey} E_y, \quad (4)$$

whereas the total energy equations for the electrons and ions separately are

$$\frac{d}{dx} \frac{5}{2} nV T_e = - n e V_e \cdot E + A \quad (5a)$$

and

$$\frac{d}{dx} \left( \frac{1}{2} nM V^3 + \frac{\gamma}{\gamma-1} nV T_i \right) = n e V_e - A, \quad (5b)$$

where  $M$  is the ion mass. The term  $A$  denotes an energy exchange between electrons and ions, and its value depends on what fraction of the resistive heating goes to electrons and what fraction goes to ions. To determine this, one must write out the temperature equations for electrons and ions. To do so, take the dot product of the electron momentum equation with  $V_e$  and subtract the result from the electron energy equation to get

$$\frac{5}{2} \frac{d}{dx} nV T_e - V \frac{d}{dx} nT_e = A + n m v_{ey}^2. \quad (6)$$

Then multiply the  $x$  component of the ion momentum equation

$$\frac{d}{dx} (nM V^2 + nT_i) = n e E \quad (7)$$

by V, subtract the results from the ion energy equation to obtain

$$\frac{5}{2} \frac{d}{dx} nV T_i - V \frac{d}{dx} nT_i = - A. \quad (8)$$

If  $\alpha$  is the ratio of ion resistive heating to electron resistive heating, then

$$\alpha = \frac{-A}{A + nmv_{ey}^2} \quad (9a)$$

or

$$A = -\frac{\alpha}{1+\alpha} nmv_{ey}^2. \quad (9b)$$

The quantity  $\alpha$  depends on the physical process causing the resistive heating. Classical resistivity gives  $\alpha \sim m/M$ . Anomalous resistivity gives an  $\alpha$  which depends upon the particular mechanism. Generally  $\alpha \ll 1$ ; for instance if the resistivity is caused by an ion acoustic instability,  $\alpha \sim 0.1-0.2$ .<sup>7,8</sup> Finally, these equations are closed by Ampere's law

$$\frac{dB}{dx} = \frac{4\pi ne}{c} v_{ey} \quad (10)$$

In order to see where the critical Mach number is, a standard procedure is to linearize Eqs. (1-10) about the upstream or downstream state. Assuming that  $\frac{d}{dx} = k$ , and an unscripted variable denotes either the upstream or downstream state, there are only two roots for  $k$ ,

k = 0

(11a)

and

$$k = \frac{\omega_{pe}^2 v}{v_c^2} \left[ \frac{v^2 - v_A^2 - \frac{\gamma T_i}{M} - \frac{5}{3} \frac{T_e}{M}}{v^2 - \frac{\gamma T_i}{M} - \frac{5}{3} \frac{T_e}{M}} \right], \quad (11b)$$

where  $v_A$  is the Alfvén speed. In our convention,  $v > 0$  so that a state with  $k > 0$  diverges from the upstream or downstream state. Notice that  $k$  is always independent of  $a$ . The reason is that all  $a$  terms are multiplied by  $v_{ey}^2$  which vanish on linearization. Further, notice that there are three ranges of velocity. First, if

$$v^2 > v_A^2 + \frac{\gamma T_i}{M} + \frac{5}{3} \frac{T_e}{M} \quad (12)$$

$k > 0$  so the linearized solution diverges away from the state. Equation (12) corresponds to the upstream state of the shock wave for which the flow speed must exceed the magnetosonic velocity. The second regime corresponds to

$$\frac{\gamma T_i}{M} + \frac{5}{3} \frac{T_e}{M} < v^2 < v_A^2 + \frac{\gamma T_i}{M} + \frac{5}{3} \frac{T_e}{M}, \quad (13)$$

where  $k < 0$ . Since the flow speed is less than the magnetosonic speed, it corresponds to the downstream state, and since  $k < 0$ , perturbations converge into the downstream state. This then is a standard (transverse) resistive shock having a subcritical Mach number. The final regime corresponds to

$$v^2 < \frac{\gamma T_i}{M} + \frac{5}{3} \frac{T_e}{M} \quad (14)$$

having  $k > 0$ . Since perturbations now diverge away from the downstream state, there can be no shock in the regime defined by Eq. (14) if transverse resistivity is the only dissipation mechanism. This then defines the critical point above which no shock can form.

To continue, let us write out the equations for a quasi-neutral shock as a system of nonlinear first order differential equations, as is appropriate for standard numerical integration.

The equations for  $B$  and  $V_{ey}$  are already expressed in the proper format in Eqs. (10) and (3). Equations (6a) and (6b) can easily be reduced to

$$\frac{dT_e}{dx} = \frac{2}{3} \left[ \frac{n m v_{ey}^2 + A}{n_o V_o} + \frac{T_e}{n} \frac{dn}{dx} \right], \quad (16)$$

and

$$\frac{dT_i}{dx} = \frac{1}{\gamma - 1} \left[ - \frac{A}{n_o V_o} + \frac{T_i}{n} \frac{dn}{dx} \right] \quad (15)$$

but now  $dn/dx$  appears on the right hand side. To solve for  $dn/dx$ , use the ion momentum equation, insert the electric field from Eq. (2), use Eqs. (15) and (16) for  $\frac{dT_E}{dx}$  and  $\frac{dT_i}{dx}$ , and solve for  $\frac{dn}{dx}$ . The result is

$$\frac{dn}{dx} = \frac{n e \frac{V_{ey}}{c} B + \frac{2}{3} \frac{n^2 m v_{ey}^2}{n_o V_o}}{M V^2 - \gamma T_i - \frac{5}{3} T_e}. \quad (17)$$

This can be used on the right hand side of Eqs. (15) and (16). Notice that  $\frac{dn}{dx}$ ,  $\frac{dT_i}{dx}$ ,  $\frac{dT_e}{dx}$  and  $E$  all become infinite at  $V^2 = (\gamma T_i + \frac{5}{3} T_e)/M$ . Thus, quasi-neutral shocks formed by transverse resistivity only exist if  $V^2 < (\gamma T_i + \frac{5}{3} T_e)/M$  everywhere. If the shock is monotonic and  $\gamma = \frac{5}{3}$  (or more generally, if  $\gamma_e = \gamma_i$ ), this critical Mach number can be determined by the Rankine-Hugoniot conditions only. However, if the shock is not monotonic, and/or  $\gamma_e \neq \gamma_i$ , the critical Mach number depends on the details of the oscillatory structure and how the resistive heating is partitioned between electrons and ions.

A key question then, for the description of shocks in the intermediate regime, is the physical significance of the singularity. One might think that the singularity indicates the onset of ion reflection, but this is not the case. To see this, imagine that  $T_i \ll T_e$ . Then ion reflection occurs where  $V \sim (T_i/M)^{1/2} \sim 0$ . However, the singularity occurs at a much higher velocity,  $V = (\frac{5T_e}{3M})^{1/2}$ . The significance of the singularity lies not in ion reflection, but rather in the breakdown of the quasi-neutral assumption. This is clear from the fact that both  $E$  and  $\frac{dE}{dx}$ , as expressed in Eq. (3), become infinite at the singularity, implying a breakdown of quasi-neutrality. Thus, in the intermediate regime, charge separation begins to play an important role in the shock structure.

### B. Shocks with Longitudinal Resistivity

In this subsection and the next, we discuss how shocks are formed by longitudinal resistivity. If quasi-neutrality is no longer assumed, the steady state ion fluid equations are

$$n_i V_i = n_o V_o \quad (18)$$

$$\frac{d}{dx} (n_i M V_i^2 + n_i T_i) = n_i e E - n_i m v_\ell (V_i - V_e), \quad (19)$$

and

$$\begin{aligned} \frac{d}{dx} \left( \frac{1}{2} m_i M V_i^3 + \frac{\gamma}{\gamma-1} n_i V_i T_i \right) &= n_i V_i e E + \frac{\alpha}{1+\alpha} n_i m v_\ell^2 \\ &+ \frac{\alpha_\ell}{1+\alpha_\ell} n_i m v_\ell (V_i - V_e)^2, \end{aligned} \quad (20)$$

where  $\alpha_\ell$  and  $v_\ell$  are defined analogously to  $\alpha$  and  $v$ . Notice that we allow different values for longitudinal and transverse dissipation and energy partition. This is reasonable because, as we will see, these two types of dissipation arise from completely different physical processes.

The fluid equations for the electrons are

$$n_e V_e = n_o V_o, \quad (21)$$

$$\frac{d}{dx} n_e T_e = - n_e e E - n_e e \frac{V_e B}{c} + n_i m v_\ell (V_i - V_e), \quad (22)$$

$$\frac{d}{dx} \frac{5}{2} n_e V_e T_e = - n_e V_e e E - n_e V_{ey} e E_y + \frac{1}{1+\alpha} n_i m v_{ey}^2 + \frac{1}{1+\alpha} n_i m v_{ly} (V_l - V_e)^2, \quad (23)$$

and

$$V_{ey} = - \frac{eV_o}{mvc} \left( B_o - \frac{n_o}{n} B \right). \quad (24)$$

These are supplemented by Maxwell's equations

$$\frac{dB}{dx} = \frac{4\pi n_e}{c} V_{ey} \quad (25)$$

and

$$\frac{dE}{dx} = 4\pi e (n_i - n_e). \quad (26)$$

As in the previous section, we begin by linearizing these equations about the upstream or downstream state. As before, there is no resistive heating in linear theory, so  $\tilde{T}_e = \frac{2}{3} T_e \frac{\tilde{n}_e}{n}$  and  $\tilde{T}_i = (\gamma-1)T_i \frac{\tilde{n}_i}{n_o}$ . Of course,  $\tilde{V}_e = - V \frac{\tilde{n}_e}{n}$  and  $\tilde{V}_i = - V \frac{\tilde{n}_i}{n}$ . Then linearizing, a straightforward calculation gives the result

$$\begin{aligned}
& k^2 (\gamma T_i - MV^2) \left( \frac{5}{3} k^2 T_e - \frac{mV \omega_c^2}{v} \frac{k^2}{k - \frac{\omega_{pe} V_o}{v c^2}} \right) \\
& - 4\pi n_o e^2 \left( 1 + \frac{v_\ell k V_o}{\omega_{pe}^2} \right) k^2 \left[ \frac{5}{3} T_e + \gamma T_i - \frac{mV_o \omega_c^2}{v} \frac{1}{k - \frac{\omega_{pe} V_o}{v c^2}} + \gamma_i T_i - MV^2 \right] = 0,
\end{aligned} \tag{27}$$

where  $\omega_c$  is the electron cyclotron frequency. Factoring out the two roots at  $k = 0$ , what remains in Eq. (27) is a cubic equation for  $k$ . As we will see, one of the roots is of order  $\omega_{pe}^2 V / v c^2$ , while the other two roots are of order  $k_D \equiv (4\pi n_e^2 / T_e)^{1/2}$ . Assuming that  $k_D \gg \omega_{pe}^2 V / v c^2$ , the equation separates. The low  $k$  root is still given by Eq. (11b). We denote this the Magnetic Mode. To get a simple form for the high  $k$  roots, we further assume that  $m\omega_c^2 / M k_D v V_o \ll 1$ , and  $\omega_c^2 / v v_\ell \ll 1$ . Since the length of a resistive shock<sup>1-5</sup> is typically  $10c/\omega_{pe}$ , an approximate order of magnitude for the anomalous collision frequency is  $v \sim 10\omega_{pe} V/c$ . The first inequality is then easily satisfied for the parameters in the experiments of Refs. (1-6, 22, 23). As for the second inequality, an estimate is required for  $v_\ell$ . As we will see in the next section,  $v_\ell$  is very large, larger even than  $\omega_{pe}$ . Thus the second inequality is also satisfied. In this case, the solution for  $k$  becomes

$$k = \frac{\frac{v_e V}{u_e^2} \left( \frac{5}{3} T_e + \gamma T_i - M V_o^2 \right)}{\frac{10}{3} (\gamma T_i - M V_o^2)} \pm$$

$$\frac{1}{\frac{10}{3} (\gamma T_i - M V_o^2)} \left[ \left( \frac{v_e V}{u_e^2} \left[ \frac{5}{3} T_e + \gamma T_i - M V_o^2 \right] \right)^2 + \frac{20}{3} k_D^2 \left( \frac{5}{3} T_e + \gamma T_i - M V_o^2 \right) (\gamma T_i - M V_o^2) \right]^{1/2}, \quad (28)$$

where  $u_e$  is the electron thermal velocity  $u_e = (T_e/m)^{1/2}$ .

Notice that the wave number given by Eq. (29) is of order  $k_D$ . Also, the magnetic field completely decouples from this large  $k$  mode, so it is entirely electrostatic in nature. Depending on the values of velocity and temperature, the linearized modes structure themselves as shown in Table I.

Now consider how to integrate Eqs. (18)-(26) to solve for the shock structures. Let us say we start upstream and integrate toward the downstream state. Referring to Table I the upstream plasma is in Class A, since the flow speed must exceed the magnetosonic speed. Hence there are two linearized perturbations which increase away from the upstream state. The relative amplitude between the two is arbitrary at this point. Now let us assume the downstream plasma is in Class B or C. In each case there are two linearized eigenfunctions which converge into the downstream state, and one which diverges. Thus the relative amplitude of the two linearized perturbations upstream must be chosen so as to eliminate the divergent perturbation downstream. This is then a nonlinear eigenvalue problem, and this concept has been applied to both conventional shocks<sup>24</sup> and reflected ion shocks.<sup>10</sup>

Table I

Velocity Regimes and linearized modes in each regime.

Class	Velocity Range	Modes
A	$MV_A^2 + \frac{5}{3} T_e + \gamma T_i < MV^2$	One electrostatic mode and the magnetic mode diverge from the state as $x$ increases in the direction of flow. The other electrostatic mode converges.
B	$\frac{5}{3} T_e + \gamma T_i < MV^2 < MV_A^2 + \frac{5}{3} T_e + \gamma T_i$	Magnetic mode converges, one electrostatic mode converges, one diverges.
C	$\gamma T_i < MV^2 < \frac{5}{3} T_e + 3T_i$	Magnetic mode diverges, both electrostatic modes converge.
D	$MV^2 < \gamma T_i$	Magnetic mode and one electric mode diverge, the other electrostatic mode converges.

If the downstream state is Class B, the scheme is trivial. The divergent downstream perturbation is electrostatic so the solution is just to eliminate electrostatics and calculate shock structure based on quasi-neutrality. If the downstream state is Class C, the problem is more complex. Here the divergent state is magnetic and both convergent states are electrostatic, so there is necessarily a coupling between the magnetic and electric structure somewhere in the shock. In the next subsection we will show how to calculate this coupled structure in a simple way by exploiting the fact that the length scale for the electric structure is very small compared to the length scale for magnetic structure.

Finally, if the downstream state is Class D, there are two divergent states downstream, but only one free parameter upstream, so that longitudinal resistivity does not allow a shock to form in this case. In the next subsection we will discuss the meaning of the singular behavior in this regime.

### C. Calculating the Double Structured Shock

As we have seen in the previous two subsections, when the plasma is making the transition from Class B to Class C, the electrostatic approximation breaks down and large electric fields and charge separations are set up by the flow. If the plasma were in Class C, and there were no dissipation, this charge separation results in an undamped ion acoustic wave. If it were in Class B with no dissipation the charge separation manifests itself as an ion acoustic soliton. With dissipation in the form of longitudinal resistivity, an ion acoustic shock can form so that the plasma can make a transition from Class B to Class C. Thus near this point, a narrow ion acoustic shock is embedded in the broader magnetic structure. This then corresponds to the isomagnetic potential jump discussed in Ref. 23.

The choice of the electrostatic wave amplitude upstream is then equivalent to a choice of the position of the ion acoustic subshock within the broader magnetic structure. As we have seen, for a Class C plasma there is no magnetic perturbation which converges into the downstream side of the ion acoustic subshock. This means for the case that  $k_D \gg \omega_{pe}^2 V/vc^2$ , where the magnetic structure and ion acoustic wave decouple, the ion acoustic wave must be at the position where the magnetic field has its downstream value.

Hence the following scheme for computing the shock structure suggests itself. First integrate the equations for a quasi-neutral resistive shock, as written in Section III.A until one reaches the position where the magnetic field has the downstream value predicted by the Rankine-Hugoniot conditions. We find that at this point, the densities and temperatures are always below the downstream values, and also  $MV^2 > 5/3 T_e + \gamma T_i$ . At this

point simply set the magnetic field equal to its constant value, set  $v_{ey} = 0$  and solve for the ion acoustic shock in the unmagnetized plasma. The equations of the ion-acoustic shock are

$$\frac{d}{dx} \left( \frac{1}{2} n_i M v_i^3 + \frac{\gamma}{\gamma-1} n_i v_i T_i \right) = n_i v_i e E + \frac{\alpha_\ell}{1+\alpha_\ell} n_i m v_\ell (v_i - v_e)^2. \quad (29)$$

The ion density and momentum equation are as in Eqs. (18) and (19). For the electrons

$$n_e V_e = n_o V_o, \quad (30)$$

$$\frac{d}{dx} n_e T_e = - n_e e E + n_i m v_\ell (v_i - v_e), \quad (31)$$

$$\frac{d}{dx} \frac{5}{2} n_e V_e T_e = - n_e V_e E + \frac{1}{1+\alpha_v} n_i m v_\ell (v_i - v_e^2), \quad (32)$$

and Poisson's Equation is still as given in Eq. (26). At the onset of the ion acoustic shock, the electric field can be initialized by taking its value from the quasi-neutral solution at the switch point. Of course, the exact value that  $E$  is initialized at is not very important because  $E$  reaches much higher values in the center of the transition region.

Then Eqs. (18, 19, 26, 29-32) are integrated from the start of the ion acoustic shock on through to the downstream state. It is easy to show that this procedure preserves the overall Rankine-Hugoniot conditions; this is shown in Appendix A.

To proceed, let us examine the singular nature of these equations by writing out equations for  $v_i$ . Eliminating  $\frac{dT_i}{dx}$  from the energy equation (Eq. (29)) and inserting it in the momentum equation, Eq. (19), we find

$$\frac{dv_i}{dx} = \frac{ev_i E - mv_\ell(v_i - v_e)[\gamma v_i - (\gamma-1) \frac{\alpha_\ell}{1+\alpha_\ell}(v_i - v_e)]}{(Mv_i^2 - \gamma T_i)} . \quad (33)$$

Now the only singularity is at  $v_i^2 = \gamma T_i / M$ . It is especially easy to draw insight from this for the case  $\gamma = 3$ , one dimensional ions. As shown in Ref. 10, the fluid equations are those derived from a waterbag ion distribution for which the thermal width is  $(3T_i/M)^{1/2}$ . Then the singularity at  $v^2 = 3T_i/M$  simply means that an ion at the outer edge of the waterbag distribution function has been reflected (its velocity has gone to zero in the shock frame). The obvious generalization then is to regard the singularity at  $v^2 = \gamma T_i / M$  as the generalization of the condition for ion reflection to two or three dimensional ion distributions. Hence this singularity does have a simple interpretation in terms of reflected ions. In Ref. 10, it was shown that for ion acoustic shocks, one could add a reflected fluid upstream. The density of this reflected fluid then becomes an additional upstream parameter, which can be varied so as to eliminate another divergent downstream solution. This might also be possible to do for the magnetosonic shocks which we consider, but it will not be examined further here.

To summarize, we have shown that longitudinal resistivity can give rise to double structured shocks in an intermediate range of Mach number. These are where the downstream state is Class C, as defined by Table 1. At the upper limit of this range, the shock structure once again becomes singular, but this singularity can now be interpreted in terms of reflected ions.

#### IV. Nonlocal Dissipation and Estimates for $v_\ell$ and $\alpha_\ell$ .

---

In the previous section, we discussed how longitudinal resistivity forms the transverse shock in the intermediate Mach number regime (Class C). The idea is that as the Mach number increases, large charge separation is generated, so an ion acoustic wave is set up. As this wave damps by longitudinal resistivity, the shock forms, as discussed in Section II. However, longitudinal resistivity is only a fluid model for the dissipation, the actual dissipation mechanism is electron or ion Landau damping, which is inherently non-fluid like. Nevertheless, it is an extremely powerful dissipative mechanism. If the ions are cold the damping distance due to electron Landau damping is extremely small, of order  $(M/m)^{1/2} k_D^{-1}$ . This implies a  $v_\ell$  of order  $\omega_{pe}$ . If the ions are warm, the Landau damping rate is larger, implying still larger values of  $v_\ell$ .

As the longitudinal resistivity appears first in the momentum equation, we proceed by calculating the term in the electron momentum equation which arises from electron Landau damping. This means getting the correction to the pressure tensor. To do so we assume the plasma is infinite and homogeneous work in the  $(\omega, \mathbf{k})$  domain, and then write a linearized fluid equation. The only term which is not completely straightforward is the pressure tensor. As usual, we denote perturbed quantities with a superscript tilda. Then

$$\tilde{f}_e = \frac{e\check{E}}{m} \frac{\frac{\partial f_e}{\partial v}}{-i\omega + ikv} \quad (34)$$

and

$$\check{f}_i = -\frac{e\check{E}}{M} \frac{\frac{\partial f_i}{\partial v}}{-i\omega + ikv}, \quad (35)$$

where now a  $v$  denotes a particle velocity in a Vlasov model and, as usual, a capital  $V$  is the fluid velocity. The total perturbed electron density is

$$\check{n}_e = \frac{e\check{E}}{m} \int \frac{\frac{\partial f_e}{\partial v}}{-i\omega + kv} = -\frac{e\check{E}n}{ikm u_e^2} [1 + \int \frac{\omega}{-\omega + kv} f_e], \quad (36)$$

where we have assumed Maxwellian electrons,  $f_e = (\sqrt{2\pi} u_e)^{-1} \exp(-v^2/2u_e^2)$  and we work now in the plasma rest frame. Taking the resonant part of the second term in the brackets of Eq. (36), that is

$$\text{Im} \frac{1}{-\omega + kv} = \pi i \delta(\omega - kv), \quad (37)$$

we find

$$\check{n}_e = -\frac{e\check{E}}{ikm u_e^2} [1 + i(\frac{\pi}{2})^{1/2} \frac{\omega}{|k|u_e}]. \quad (38)$$

To continue, we would like to find the perturbed part of the total electron momentum flux

$$\check{p}_e = m \int dv v^2 \check{f}_e = -\frac{e\check{E}}{u_e^2} \int dv v^3 \frac{f}{-i\omega + ikv}. \quad (39)$$

The resonant part is small by a factor of  $(\frac{\omega}{ku_e})^3$  and we neglect it, so that

$$\check{p}_e = -\frac{e\check{E}}{ik} n. \quad (40)$$

To obtain an equation of state, we need the perturbed pressure in terms of the perturbed density. From Eqs. (38) and (40) we find

$$\check{P}_e \approx T_e [1 - i\sqrt{\frac{\pi}{2}} \frac{\omega}{k u_e} \frac{k}{|k|}] \check{n}_e. \quad (41)$$

The force on the electrons is  $-ik\check{P}_e$ . The first term in the square brackets simply gives  $-T_e \frac{\partial}{\partial x} \check{n}_e$ , the pressure gradient force on an isothermal plasma. The second term, which is out of phase by  $\pi/2$  is the additional dissipative contribution to the electron force. Using the fact that the linearized density equation gives the result  $n\check{V}_e = \omega/k \check{n}_e$ , we find the additional force density on the electrons is

$$\check{F}_e = -ik\check{P}_e = -ikT_e \check{n}_e - n m u_e \sqrt{\frac{\pi}{2}} \frac{k^2}{|k|} \check{V}_e. \quad (42)$$

Modeling this additional retarding force as a longitudinal resistivity in the subshock, we find

$$v_\ell \sim \omega_{pe} \quad (43)$$

where we have assumed that within the subshock  $k \sim k_D$ .

Although the dissipation from Landau damping is quite simple in the  $k$  domain, it is very complicated and nonlocal in the  $x$  domain. In the  $k$  domain, the dissipative part of the perturbed pressure is the product of  $-i nm u_e \sqrt{\frac{\pi}{2}} \frac{k}{|k|}$  and  $\check{V}_e$ . In the  $x$  domain, it is the convolution of the Fourier transforms of the two factors. Thus the dissipative part of the perturbed pressure in the  $x$  domain is

$$\check{P}_{ed} = n m u_e \sqrt{\frac{\pi}{2}} P \int dx' \frac{\check{V}_e(x')}{x-x'} \quad (44)$$

where  $P$  denotes the principal value.<sup>25</sup> Thus the actual dissipation is nonlocal and quite complicated.

Now we consider the dissipative force on the ions. An exact analog of the calculation leading up to Eq. (42) gives the result that the dissipative force density on the ion fluid is given by

$$\check{F}_{id} = \pi M(\omega/k)^3 \frac{k^2}{|k|} \frac{\partial f_i}{\partial v}|_{\omega/k} \check{V}_i. \quad (45)$$

For the case of positive phase velocity,  $\frac{\partial f_i}{\partial v}|_{\omega/k} < 0$  for a thermal ion distribution, so that the force is still a retarding force. Assuming  $\omega/k$  is roughly constant as a function of  $k$ , the perturbed ion pressure in the  $x$  domain has the same form as given in Eq. (45). Depending on the ion temperature, the  $v_\ell$  corresponding to the ion Landau damping can be large or small. If the electron temperature is comparable to the ion temperature, the damping length is comparable to  $k_D^{-1}$ , implying that  $v_{\ell i} \lesssim (\frac{M}{m})^{1/2} \omega_{pe}$ . Hence for either electron or ion dissipation, values for  $v_\ell$  are quite large, easily large enough that the electrostatic potential is highly localized in the overall magnetic structure. Furthermore, the dissipation is not anomalous, in the sense that it does not arise from any instability, as does the dissipation which generates the transverse  $v$ .

Since ion Landau damping heats the ions, and electron Landau damping heats the electrons, a reasonable guess for  $\alpha_\ell$  is

$$\alpha_\lambda \sim \frac{\sqrt{2\pi}^1 MV^3 \frac{\partial f}{\partial v} \Big|_{v=v}}{n m u_e} \quad (46)$$

where we have taken  $\omega/k = V$ , the flow speed.

We now continue this section by discussing other aspects of the Landau damping model. As complicated as say Eq. (44) for  $\check{P}_{ed}$  is, it is still a fairly coarse approximation to the actual nonlocal dissipation for several reasons. First of all, Eq. (44) is derived from linear theory, whereas the shock wave is inherently nonlinear. Secondly, since it is nonlocal, perturbed velocities everywhere contribute to the perturbed dissipative pressure at each point. However, only a portion of the plasma is electrostatic; a large part of it is dominated by the magnetic structure, and this was not treated correctly at all in the calculation of  $\check{P}_{ed}$ . Third, the Fourier transform technique used to calculate  $\check{P}_e$  works only if  $\check{P}_e$  is either periodic or square integrable. However, a shock profile is neither so it is not clear just how valid the Fourier representation is. For instance, if  $\check{V}_e(x)$  in Eq. (44) has a typical shock structure, then the integral in Eq. (44) diverges for large  $x$ . Thus the linear theory in the Fourier domain gives an infinite perturbed pressure at large  $x$ , that is, the region of  $x$  furthest from the shock. It is the divergence which is at the root of the claim by Pfirsch and Sudan<sup>26</sup> that Landau damping cannot form a steady state shock. We feel that this divergence is clearly unphysical, so either nonlinear contributions play an important role in determining  $\check{P}_e$  or else the Fourier transform scheme must be modified.

Hence, since the actual dissipation mechanism is so complicated, a simple fluid approximation to it could be extremely useful. The only four possible conventional dissipation mechanisms are thermal conductivity, viscosity, transverse resistivity, and longitudinal resistivity. Thermal

conduction can almost certainly be eliminated as a mechanism to form the shock because there does not seem to be any way that diffusing temperature can slow the forward motion and turn the upstream kinetic energy into downstream temperature. Viscosity can form the shock. However, there is no maximum Mach number for a viscous shock, no way that it is related to the breakdown of quasi-neutrality, and no way that it is related to ion reflection. Since all of these are known to be important in experiments, viscosity does not appear to be the best fluid description of the dissipation either. Transverse resistivity is not only a good approximation, in all likelihood it is the dissipation mechanism, since transverse electron-ion streaming can give rise to instabilities which exchange momentum between electrons and ions.<sup>7</sup> However, as we have seen, transverse resistivity can only form the shock for Class B plasmas.

This leaves longitudinal resistivity. While the actual dissipation mechanism is considerably more complex than this, it is a very good approximation to the physics. It is directly related to the breakdown of quasi-neutrality, it has an upper Mach number limit corresponding to ion reflection, it predicts a very narrow isomagnetic potential jump at the shock crest, and it has a lower Mach number limit corresponding to the maximum Mach number for transverse resistivity. All of these features are confirmed by the laboratory experiments we have cited. Furthermore, while longitudinal resistivity is simple, the two parameters which characterize it,  $v_L$  and  $\alpha_L$  can be estimated from a coarse approximation to the actual dissipation mechanism.

Let us conclude this section by discussing an important additional constraint on the physics. As we have seen, our basic model is that the flow steepens up until an ion acoustic wave is generated. The Landau

damping of this ion acoustic wave then provides the dissipation which forms the shock. However, for the theory of Landau damping to be valid,<sup>27</sup> the trapping time (for say the ions)

$$\tau_T \sim k \left(\frac{e\phi}{M}\right)^{1/2}, \quad (47)$$

where  $\phi$  is the electrostatic potential, must be longer than the correlation time for a particle with velocity  $v$ .

$$\tau_c = \frac{k \sum |E(k)|^2 \delta(kv-\omega)}{\sum |E(k)|^2} . \quad (48)$$

However, if the shock is simply a steady state potential profile,  $\tau_c = \infty$  for particles at the shock velocity. Hence the entire concept of Landau damping breaks down and the ion dynamics is dominated by trapping in a stationary potential. Thus in order for the Landau damping model to be valid, either the shock must have a temporally fluctuating structure, or else the total time of the experiment must be less than a trapping time. It is very likely that the shocks do have a fluctuating structure if only because in the broader part, dominated by transverse resistivity, the resistivity is probably caused by Debye length scale streaming instabilities. The spectrum of unstable waves will almost certainly overlap the electrostatic subshock and give rise to overall fluctuations in time.

## V. Results

In this section we present results of the calculations outlined in Section III. There are two classes of calculations. First, we consider parameters like those examined experimentally in Ref. 22. Here we model the longitudinal resistive heating as going entirely into the ions, as would be the case for strong ion Landau damping (that is  $T_i$  not much less than  $T_e$ ). Secondly, we consider a nitrogen plasma with parameters like that given in Ref. 21. More important, however, we consider no resistive ion heating.

### A. The Case of Strong Ion Heating

In this case, we consider a shock in a hydrogen plasma with parameters as given in Ref. 22. That is, the upstream density is  $4.6 \times 10^{14} \text{ cm}^{-3}$  and the upstream field is 730G. The ion  $\gamma$  is taken as equal to 5/3, and  $T_e = T_i = 1 \text{ ev}$ . As is conventional in resistive shocks we assume a length of roughly  $10 c/\omega_{pe}$  so that  $cV/\omega_{pe} V_A = 10$  where we use upstream values for the plasma frequency and Alfvén speed. Although it is often assumed that for transverse resistive shocks there is no resistive ion heating, it is not easy to envision a transverse streaming instability which gives none. Also, a small amount of resistive ion heating would be extremely difficult to measure, and it might in fact be very important in determining the resistive shock width.<sup>8</sup> In addition, the ion temperature greatly affects the ion Landau damping rate in the electrostatic portion of the shock. Accordingly we take  $\alpha = 0.2$ , so there is 5 times as much resistive electron heating as resistive ion heating in the transverse part of the shock.

Since the transverse resistive shock always has a monotonic structure, the critical Mach number for transition to the Class C downstream state can be determined from the Rankine-Hugoniot conditions. For the parameters cited, this critical Mach number turns out to be 2.64. (Here the Mach number is defined as the shock velocity divided by the upstream magnetosonic speed). For Mach numbers below this, the shock is quasi-neutral and its structure is determined as specified in Section III.A.

Above this Mach number, the quasi-neutral assumption breaks down. For larger Mach numbers, the shock structure is calculated as described in Secs. III.B and C. We assume, as seems consistent with experimental data, that in the electrostatic portion, ion Landau damping dominates. Thus we take  $\alpha_l = \infty$  and  $v_l = \frac{1}{2} \left(\frac{M}{m}\right)^{1/2} \omega_{pe}$ . The upper critical Mach number, the transition from Class C to Class D cannot be determined from Rankine-Hugoniot conditions alone for two reasons. First of all the electrostatic part of the shock generally is not monotonic, but overshoots the final density, and then decays down to the downstream value. Secondly, even if the shock were monotonic, the Rankine-Hugoniot condition gives only  $T_e + T_i$ , whereas the transition from Class C to Class D depends only on  $T_i$ . Therefore this upper critical Mach number depends on how the resistive heating is partitioned between electrons and ions. For the parameters we have chosen, we find that this upper critical Mach number turns out to be about 4.46. This agrees reasonably well with the upper limit Mach number of  $4.25 \pm 0.2$  in Ref. 22. In Figs. 1a and 1b are shown magnetic field and density profiles for a Class B shock with  $m = 2.5$ . Distances are given in centimeters. In Fig. 2a and 2b are shown magnetic field and density profiles in the transverse part of a supercritical shock having  $m = 4.4$ . The transverse part ends when the magnetic field achieves its downstream

value. At this point the electrostatic subshock is excited. The electron and ion density as a function of  $x$  in this region is shown in Fig. 2c. Again, distances are in centimeters. In all calculations, downstream values are carefully compared with Rankine-Hugoniot conditions as an independent check on the calculations.

The actual ion heating downstream was measured in Ref. 22 by measuring  $n_e(T_e + T_i)$  magnetically, and then measuring  $n_e$  and  $T_e$  by laser scattering. The results, along with our calculated results, are shown in Fig. 3. The two basically agree, although the experiment shows somewhat more ion heating than what is calculated.

Another important experimental result from Ref. 23 is that as the Mach number increases, the value of  $2e\phi/M(V_o^2 - V_d^2)$  decreases. Here  $\phi$  is the total potential jump and  $V_o$  and  $V_d$  are upstream and downstream flow speeds. This goes hand in hand with the idea that as the Mach number increases, ions are slowed down not only by the electric field, but also by some additional dissipative effect. Our dissipative model, longitudinal resistivity also provides additional ion slowing down. In Fig. 4 are shown variations of this parameter with Mach number as measured by Eselevich et al., and as we calculated assuming upstream parameters in Ref. 22. Again the agreement is quite good.

#### B. Shocks with No Ion Heating

In this section we consider shocks with no ion heating,  $\alpha = \alpha_\lambda = 0$ . This corresponds to zero temperature ions, or else a waterbag ion distribution in one dimension. We consider the latter, so  $\gamma_i = 3$ . Since the electrons and ions have different values of  $\gamma$ , the Rankine-Hugoniot conditions cannot be calculated in the conventional way. However, by making use of the fact that  $\alpha = 0$ , and the ions only heat adiabatically,

the conservation relations can be calculated. This is done in Appendix C. For upstream fluid parameters, we use those in Ref. 21, a singly ionized nitrogen plasma,  $n = 10^{15}$ ,  $B = 2\text{KG}$ ,  $T_e = 2 \text{ ev}$ ,  $T_i = 0.5 \text{ ev}$ ,  $c\nu/\omega_{pe}V_A = 10$ , and  $\nu_\ell = \omega_{pe}$ , corresponding to electron-Landau damping. Then, Rankine-Hugoniot conditions show that the Mach number for transition from Class B to Class C is  $M = 2.68$ . There is no second critical Mach number for transition from Class C to Class D predicted by Rankine-Hugoniot simply because there is not enough ion heating. However, the shock is not monotonic, but oscillatory, so that in an overshoot it is possible to reach the second critical point  $V^2 = 3T_i/M$ . We find this singular point is reached at  $m = 3.73$ . In Fig. 5a and 5b are shown magnetic field and density profiles versus position in the quasi-neutral part for a shock with  $m = 3.5$ . In Fig. 5c is the ion density versus  $x$  in the electrostatic part.

## VI. Conclusions

Our first conclusion is that the experimental evidence strongly indicates the existence of a significant intermediate range of Mach numbers between shocks formed by transverse resistivity and shocks formed by reflected ions. In this range, according to Ref. 23, the breakdown of quasi-neutrality plays an important role and an electrostatic subshock forms on the crest of the magnetic structure. Second, we have shown that the singular behavior of the quasi-neutral fluid equations is not related to ion reflection but rather to the breakdown of quasi-neutrality. In the intermediate regime then, an ion acoustic wave train is set up. We speculate that the Landau damping of this acoustic wave is the dissipation mechanism which forms the shock. Third, we have investigated longitudinal resistivity as a simple fluid model for the dissipation mechanism for shock formation. We conclude that it is a reasonable model. It is important only between the upper Mach number for transverse resistivity, and the lower Mach number for a fluid picture of ion reflection. It also is directly related to the breakdown of the quasi-neutrality assumption, and it predicts an electrostatic subshock at the crest of the magnetic structure.

## Acknowledgment

This research was supported by the Defense Nuclear Agency.

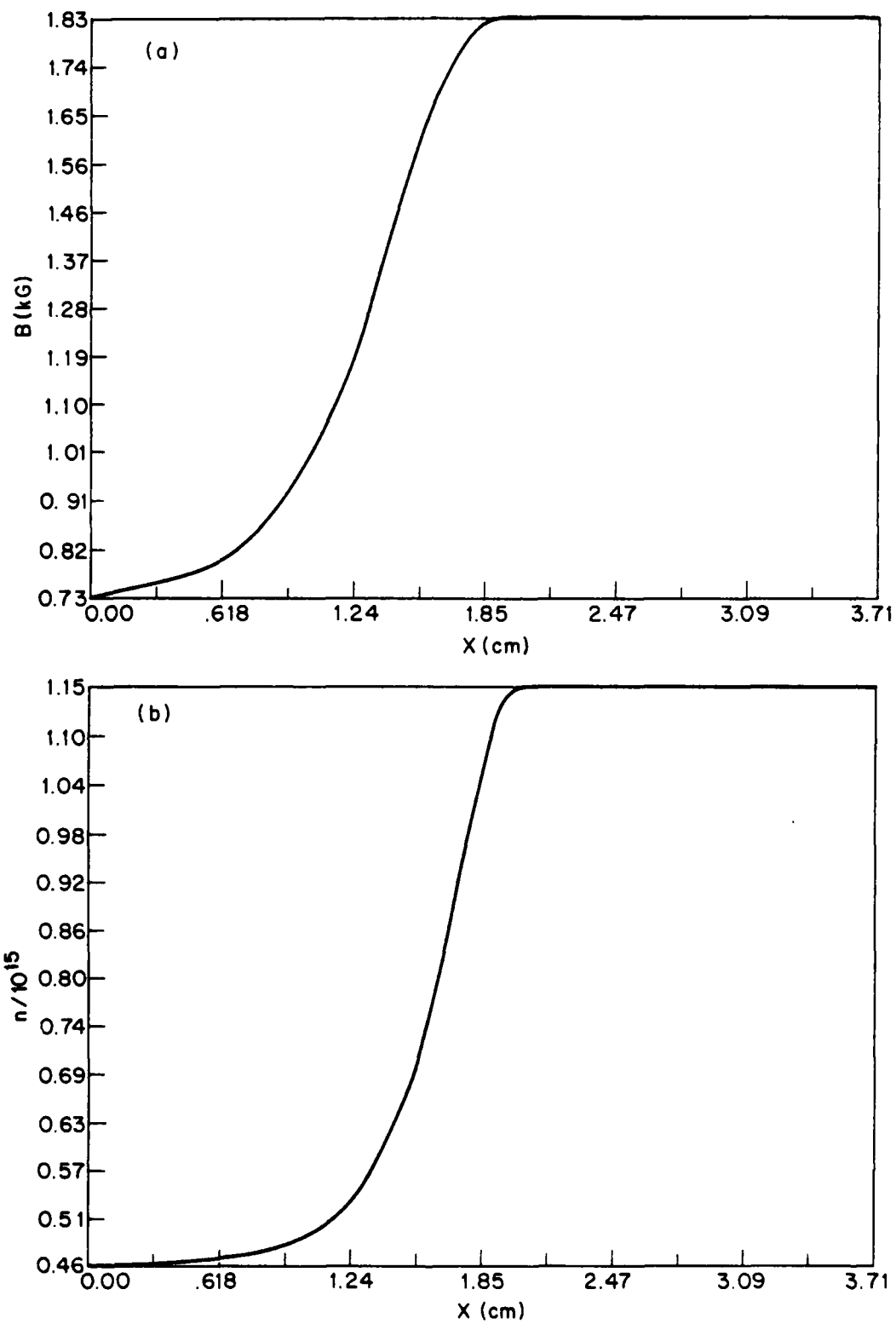


Figure 1 a) Magnetic field and, b) density profile for a subcritical shock with  $m = 2.5$ .

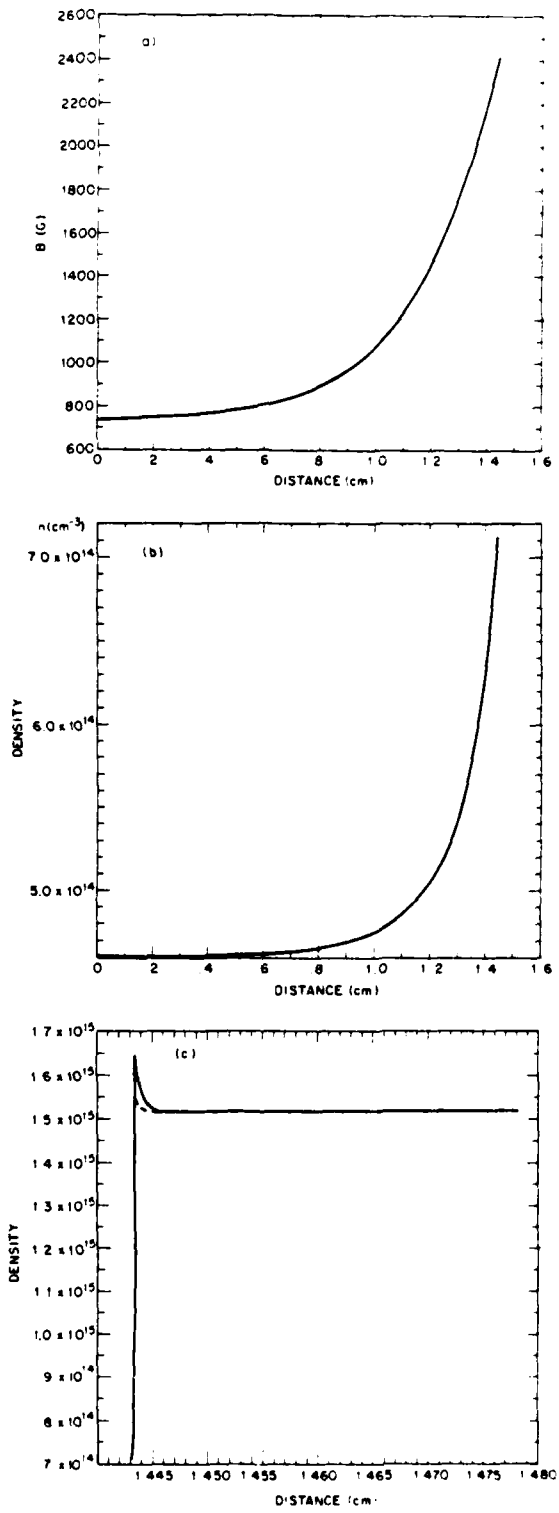


Figure 2 a) Magnetic field and, b) density profiles in the transverse part of the supercritical shock having  $m = 4.4$ . c) Ion (solid) and electron (dotted) density profile in the electrostatic part of the shock.

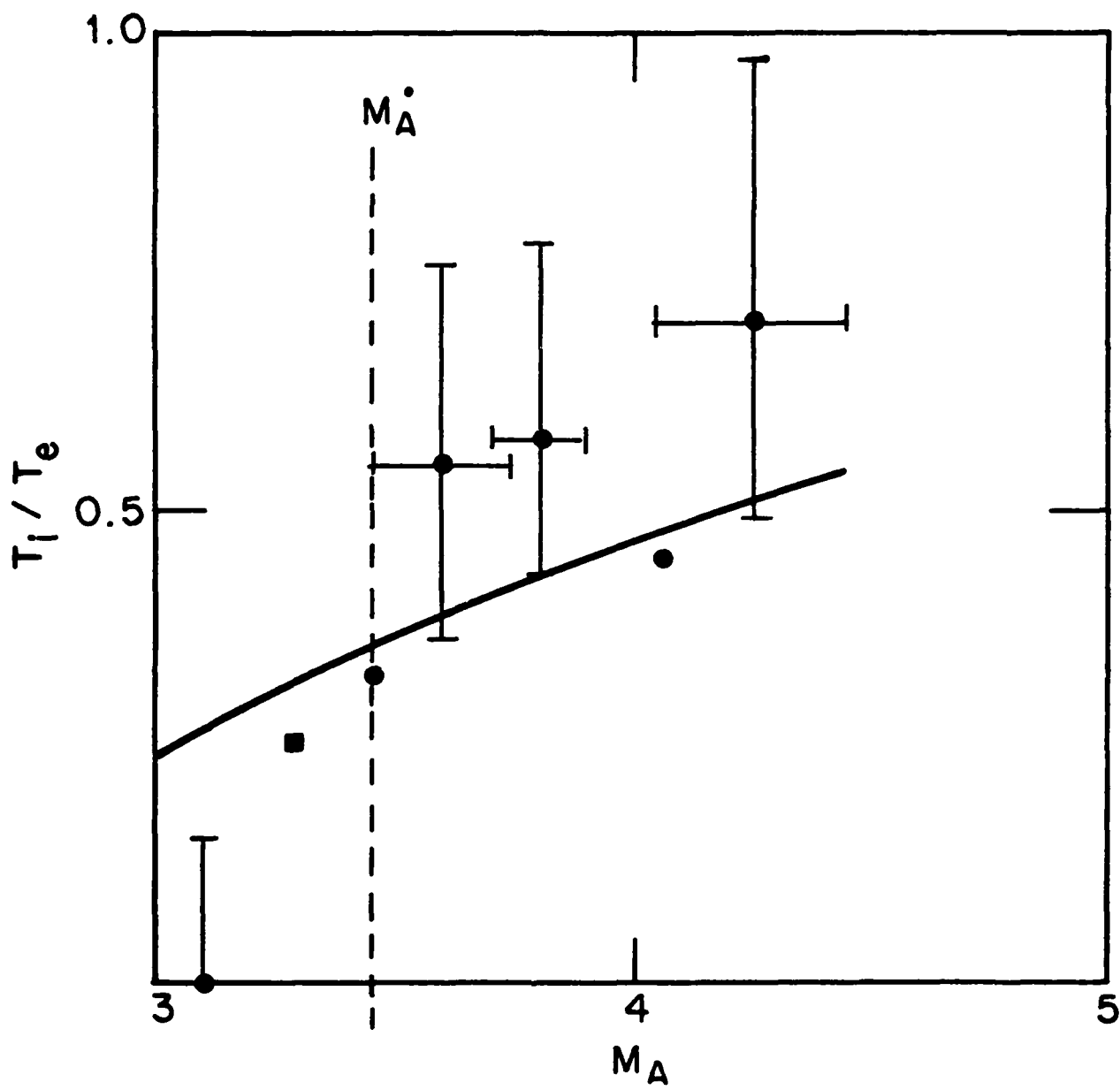


Figure 3. Calculated and measured downstream ion temperatures for intermediate range shocks as a function of  $m$ .

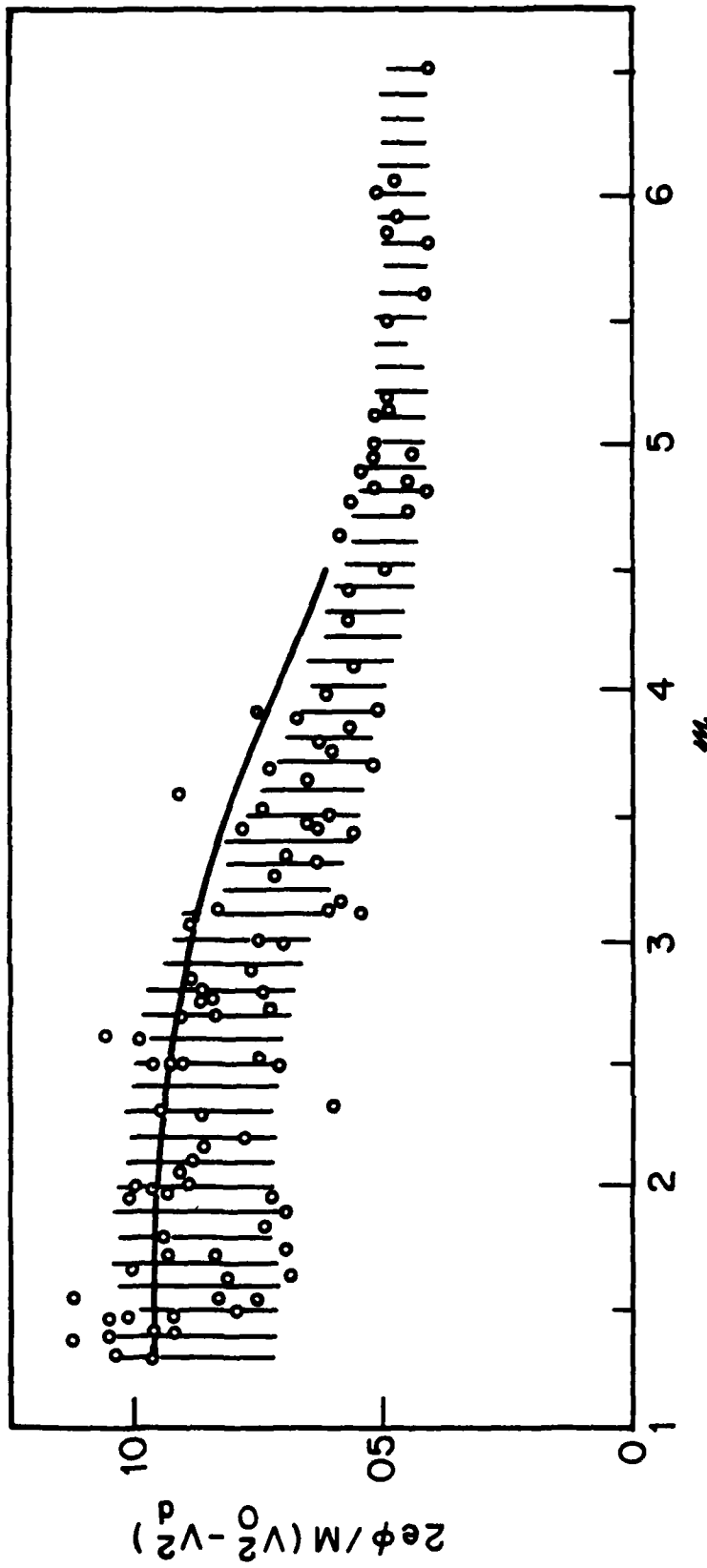
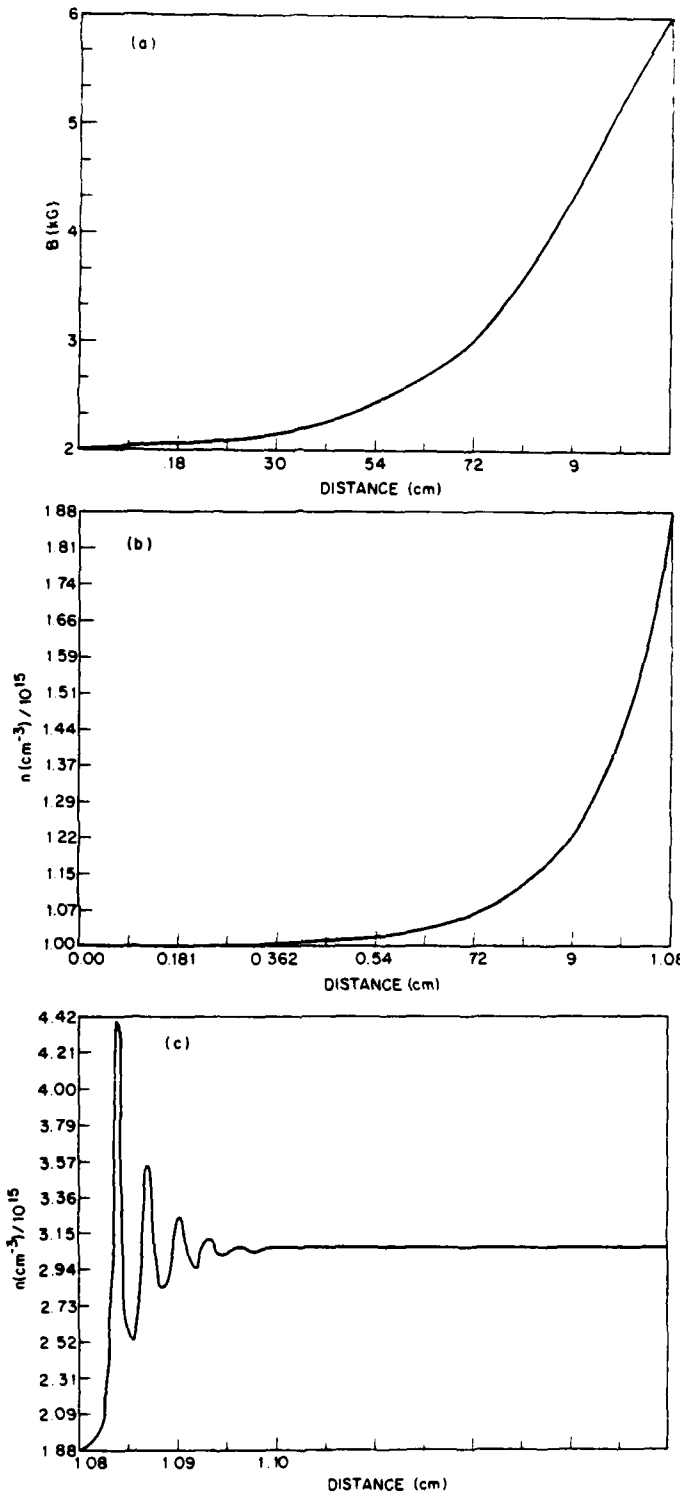


Figure 4 Calculated (solid heavy line) and measured values of  
 $2e\phi/M(V_0^2 - V_d^2)$  as a function of  $m$ .



**Figure 5** a) Magnetic field and, b) density in the transverse part of a shock with no ion heating. c) Ion density in the electrostatic region.

## Appendix A

In this appendix, we show that the scheme for determining the shock structure, as specified in Section III.C satisfy the overall conservation relations. Three of the conservation relations, that for mass, momentum and energy are satisfied at each point in the shock. The fourth relation  $uB = U_0 B_0$  is only satisfied downstream.

Consider now the conservation equations for momentum and energy flux. Each flux is the sum of a fluid and electromagnetic component. In the quasi-neutral region, the electrostatic part of the momentum flux is neglected, but the magnetic part of the momentum flux,  $B^2/8\pi$  and the electromagnetic part of the energy flux  $\frac{c}{4\pi} BE_0$  are each included in the formulation. In the quasi-neutral region then, n, V, and T are determined, in part, so that particle, momentum and total energy flux are conserved. At the switch point, B takes on its downstream value and remains constant. Therefore in the electrostatic region, the magnetic part of the momentum flux and electromagnetic part of the energy flux are constant and have the proper downstream value.

In the electrostatic region, the formulation leads to a conservation law for total energy flux and a conservation law for total fluid momentum flux plus electrostatic momentum flux -  $\frac{E^2}{8\pi}$ . Downstream, of course,  $E = 0$  and the fluid momentum and energy fluxes are as given by the Rankine-Hugoniot condition.

Now consider the fluid energy flux as one moves back upstream toward the switch point in the electrostatic region. Since it is constant, it matches smoothly onto that in the quasi-neutral regime. Next consider the momentum flux. Since the formulation for the electrostatic region contains

a momentum flux -  $\frac{E^2}{8\pi}$ , and the quasi-neutral formulation does not, the momentum fluxes do not quite match at the switch point if they have the same values downstream. However, if  $\frac{E^2}{8\pi}$  is a very small part of the momentum flux at the switch point, the error in momentum flux is very small. Using the expression for E at the switch point, Eq. (2), and considering say the ratio of electrostatic to thermal momentum flux, we find  $\frac{E^2}{8\pi}/nT_e \sim (\omega_{pe}^2 v/vc^2 k_D)^2 \ll 1$ . In all of our calculations of shock structure, we have checked that the electrostatic component of the momentum flux is negligible at the switch point, so that total momentum is conserved throughout the shock. Of course, while the electrostatic momentum flux is very small at the beginning and end of the electrostatic shock, it can be very large at points in between.

## Appendix B

In this appendix, we calculate Rankine-Hugoniot conditions for the case of  $\gamma_e = \frac{5}{3}$ ,  $\gamma_i = 3$ , but where the ions are only heated adiabatically so that  $T_i = T_{io} \left(\frac{n}{n_o}\right)^2$ . Then denoting upstream quantities with a subscript zero and downstream quantities with no subscript, the conservation equations for momentum and energy flux reduce to two equations for  $n$  and  $T_e$ .

$$n_o MV_o^2 + n_o (T_{eo} + T_{io}) + \frac{B_o^2}{8\pi} = \frac{n_o^2 MV_o^2}{n} + n T_e + \frac{T_{io}}{n_o^2} n^3 + \frac{B_o^2}{8\pi} \left(\frac{n}{n_o}\right)^2 \quad (B1)$$

$$\frac{MV_o^2}{2} + \frac{5}{2} T_{eo} + \frac{3}{2} T_{io} + \frac{B_o^2}{4\pi n_o} = \frac{MV_o^2 n_o^2}{n^2} + \frac{5}{2} T_e + \frac{3}{2} T_{io} \left(\frac{n}{n_o}\right)^2 + \frac{B_o^2 n}{4\pi n_o^2} \quad (B2)$$

In writing Eqs. (B1) and (B2) we have used the fact that  $n_o V_o = nV$  and  $V_o B_o = VB$ . Now each equation is linear in  $T_e$ , so solving for  $T_e$  from one and inserting in the other, we find

$$\begin{aligned} MV_o^2 \left(1 - \frac{1}{u}\right) + T_{io} \left(1 - u^3\right) + \frac{MV_{Ao}^2}{2} \left(1 - u^2\right) + (1 - u) T_{eo} = \\ \frac{2}{5} u \left[ \frac{MV_o^2}{2} \left(1 - \frac{1}{u^2}\right) + \frac{3}{2} T_{io} \left(1 - u^2\right) + MV_{Ao}^2 \left(1 - u\right) \right] \end{aligned} \quad (B3)$$

where  $u = \frac{n}{n_o}$  and  $V_{Ao}^2 = B_o^2 / 4\pi n_o M$ . Factoring out the obvious root  $u = 1$ , we arrive at a cubic equation for  $u$

$$\begin{aligned} - \frac{MV_o^2}{u} + T_{io} \left(1 + u + u^2\right) + \frac{MV_{Ao}^2}{2} \left(1 + u\right) + T_{eo} = \\ \frac{2}{5} u \left[ - \frac{MV_o^2}{2u^2} \left(1 + u\right) + \frac{3}{2} T_{io} \left(1 + u\right) + MV_{Ao}^2 \right]. \end{aligned} \quad (B4)$$

This equation also has a root  $u = 1$  if  $MV_o^2 = MV_{Ao}^2 + \frac{5}{3} T_{eo} + 3T_i$  as can be easily verified. The procedure then is to solve Eq. (B4) numerically starting from this root and following it as  $V_o$  increases. Assuming a singly ionized nitrogen plasma with  $n_o = 10^{15}$ ,  $T_{eo} = 2\text{ev}$ ,  $T_{io} = 0.5\text{ev}$ ,  $B = 2\text{KG}$ , Fig. B1 shows a plot of downstream values of density and electron temperature versus magnetosonic Mach number  $m = V_o / (V_{Ao}^2 + \frac{5}{3} T_{eo}/M + 3T_{io}/M)^{1/2}$ .

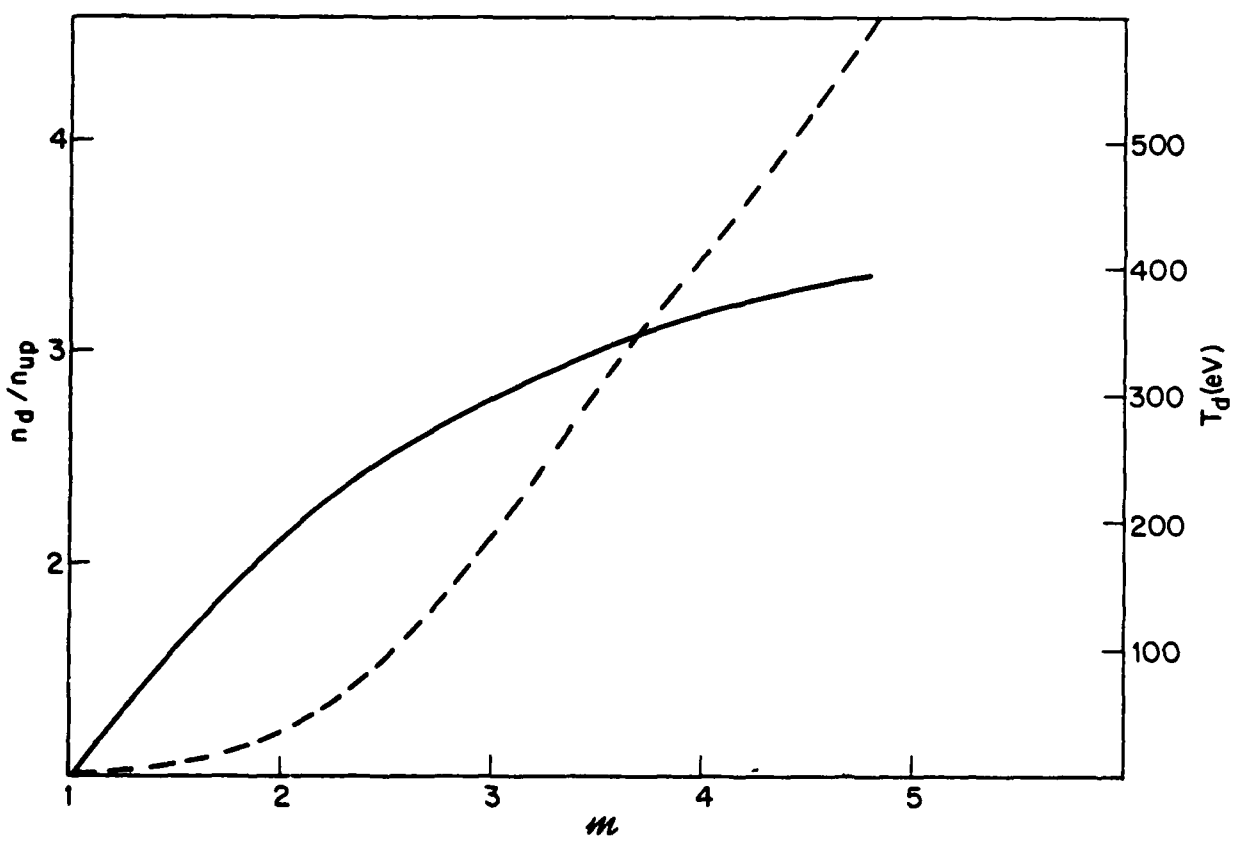


Figure B1 Downstream electron temperature (dotted) and density ratio (solid) for a shock with  $\gamma_e = 5/3$ ,  $\gamma_i = 3$  and adiabatic ion heating.

### References

- 1) J.W.M. Paul, L.S. Holmes, M.J. Parkinson and J. Sheffield, *Nature* 208, 133 (1965).
- 2) J.W.M. Paul, G.C. Goldenbaum, A. Iiyoshi, L.S. Holmes and R.A. Hardcastle, *Nature* 216, 363 (1967).
- 3) M. Keilhacker, M. Kornherr, H. Niedermeyer, K.-H. Steuer and R. Chodura, *Plasma Physics and Controlled Nuclear Fusion Research 1971*, Vol. 3, p. 265, IAEA, Vienna, 1972.
- 4) P. Bogen, K.J. Dietz, K.H. Dippel, E. Hintz, K. Hothker, F. Siemsen and G. Zeyer, *Ibid*, p. 277
- 5) V.G. Eselevich, A.G. Eskov, R.Kh. Kurtmullaev, A.I. Malyutin, Sov. Phys. *JETP*, 33, 898 (1971).
- 6) R.M. Perkin, A.D. Craig, L.S. Holmes, and J.M.W. Paul, *Plasma Physics and Controlled Nuclear Fusion Research 1974*, Vol. 2, p. 681, IAEA, Vienna, 1975.
- 7) M. Lampe, W.M. Manheimer, J.B. McBride, J.H. Orens, K. Papadopoulos, R. Shanney, and R.N. Sudan, *Phys. Fluids*, 15, 662 (1972).
- 8) Wallace M. Manheimer and J.P. Boris, *Phys. Rev. Lett.*, 28, 659 (1972).
- 9) D.W. Forslund and J.P. Freidberg, *Phys. Rev. Lett.*, 27, 1189 (1971).
- 10) W.M. Manheimer and I. Haber, *Phys. Fluids*, 17, 706 (1974).
- 11) M.M. Leroy, *Phys. Fluids*, 26, 2742 (1983).
- 12) D.W. Forslund and C.R. Shonk, *Phys. Rev. Lett.*, 25, 1699 (1970).
- 13) P.H. Sakanaka, C.K. Chu and T.C. Marshall *Phys. Fluids*, 14, 611 (1971).
- 14) K. Papadopoulos, C.E. Wagner, and I. Haber, *Phys. Rev. Lett.*, 27, 982 (1971).
- 15) R.J. Mason, *Phys. Fluids*, 15, 1082 (1972).

- 16) D. Biskamp and H. Welter, J. Geophys. Res., 77, 6052 (1972).
- 17) D. Biskamp and H. Welter, Nucl. Fusion, 12, 663 (1972).
- 18) M.M. Leroy, C.C. Goodrich, D. Winske, C.S. Wu, and K. Papadopoulos, Geophys. Res. Lett., 8, 1269 (1981).
- 19) M.M. Leroy, D. Winske, C.C. Goodrich, C.S. Wu and K. Papadopoulos, J. Geophys. Res., 87, 5081 (1982).
- 20) R.J. Taylor, D.R. Baker and H. Ikezi, Phys. Rev. Lett., 24, 206 (1970).
- 21) B.H. Ripin, to be published.
- 22) S.E. Segre and M. Martone, Plasma Phys., 13, 113 (1971).
- 23) V.G. Eselevich, A.G. Eskov, R.Kh. Kurtmullaev, and A.I. Malyutin, Sov. Phys. JETP, 33, 898 (1971).
- 24) L.C. Woods, Plasma Phys., 11, 25 (1969).
- 25) E. Ott and R.N. Sudan, Phys. Fluids, 12, 2388 (1969).
- 26) D. Pfirsch and R.N. Sudan, Phys. Fluids, 14, 1033 (1971).
- 27) T.H. Dupree, Phys. Fluids, 9, 1773 (1966).

DISTRIBUTION LIST

DEPARTMENT OF DEFENSE

ASSISTANT SECRETARY OF DEFENSE  
COMM, CMD, CONT 7 INTELL  
WASHINGTON, D.C. 20301

DIRECTOR  
COMMAND CONTROL TECHNICAL CENTER  
PENTAGON RM BE 685  
WASHINGTON, D.C. 20301  
01CY ATTN C-650  
01CY ATTN C-312 R. MASON

DIRECTOR  
DEFENSE ADVANCED RSCH PROJ AGENCY  
ARCHITECT BUILDING  
1400 WILSON BLVD.  
ARLINGTON, VA. 22209  
01CY ATTN NUCLEAR MONITORING RESEARCH  
01CY ATTN STRATEGIC TECH OFFICE

DEFENSE COMMUNICATION ENGINEER CENTER  
1860 WIEHLE AVENUE  
RESTON, VA. 22090  
01CY ATTN CODE R410  
01CY ATTN CODE R812

DEFENSE TECHNICAL INFORMATION CENTER  
CAMERON STATION  
ALEXANDRIA, VA. 22314  
02CY

DIRECTOR  
DEFENSE NUCLEAR AGENCY  
WASHINGTON, D.C. 20305  
01CY ATTN STVL  
04CY ATTN TITL  
01CY ATTN DDST  
03CY ATTN RAAE

COMMANDER  
FIELD COMMAND  
DEFENSE NUCLEAR AGENCY  
KIRTLAND, AFB, NM 87115  
01CY ATTN FCPR

DIRECTOR  
INTERSERVICE NUCLEAR WEAPONS SCHOOL  
KIRTLAND AFB, NM 87115  
01CY ATTN DOCUMENT CONTROL

JOINT CHIEFS OF STAFF  
WASHINGTON, D.C. 20301  
01CY ATTN J-3 WWMCCS EVALUATION OFFICE

DIRECTOR  
JOINT STRAT TGT PLANNING STAFF  
OFFUTT AFB  
OMAHA, NB 68113  
01CY ATTN JLTW-2  
01CY ATTN JPST G. GOETZ

CHIEF  
LIVERMORE DIVISION FLD COMMAND DNA  
DEPARTMENT OF DEFENSE  
LAWRENCE LIVERMORE LABORATORY  
P.O. BOX 808  
LIVERMORE, CA 94550  
01CY ATTN FCPR

COMMANDANT  
NATO SCHOOL (SHAPE)  
APO NEW YORK 09172  
01CY ATTN U.S. DOCUMENTS OFFICER

UNDER SECY OF DEF FOR RSCH & ENGRG  
DEPARTMENT OF DEFENSE  
WASHINGTON, D.C. 20301  
01CY ATTN STRATEGIC & SPACE SYSTEMS (OS)

WWMCCS SYSTEM ENGINEERING ORG  
WASHINGTON, D.C. 20305  
01CY ATTN R. CRAWFORD

COMMANDER/DIRECTOR  
ATMOSPHERIC SCIENCES LABORATORY  
U.S. ARMY ELECTRONICS COMMAND  
WHITE SANDS MISSILE RANGE, NM 88002  
01CY ATTN DELAS-EO F. NILES

DIRECTOR  
BMD ADVANCED TECH CTR  
HUNTSVILLE OFFICE  
P.O. BOX 1500  
HUNTSVILLE, AL 35807  
01CY ATTN ATC-T MELVIN T. CAPPS  
01CY ATTN ATC-O W. DAVIES  
01CY ATTN ATC-R DON RUSS

PROGRAM MANAGER  
BMD PROGRAM OFFICE  
5001 EISENHOWER AVENUE  
ALEXANDRIA, VA 22333  
01CY ATTN DACS-BMT J. SHEA

CHIEF C-E- SERVICES DIVISION  
U.S. ARMY COMMUNICATIONS CMD  
PENTAGON RM 1B269  
WASHINGTON, D.C. 20310  
01CY ATTN C- E-SERVICES DIVISION

COMMANDER  
FRADCOM TECHNICAL SUPPORT ACTIVITY  
DEPARTMENT OF THE ARMY  
FORT MONMOUTH, N.J. 07703  
01CY ATTN DRSEL-NL-RD H. BENNET  
01CY ATTN DRSEL-PL-ENV H. BOMKE  
01CY ATTN J.E. QUIGLEY

COMMANDER  
U.S. ARMY COMM-ELEC ENGRG INSTAL AGY  
FT. HUACHUCA, AZ 85613  
01CY ATTN CCC-EMEO GEORGE LANE

COMMANDER  
U.S. ARMY FOREIGN SCIENCE & TECH CTR  
220 7TH STREET, NE  
CHARLOTTESVILLE, VA 22901  
01CY ATTN DRXST-SD

COMMANDER  
U.S. ARMY MATERIAL DEV & READINESS CMD  
5001 EISENHOWER AVENUE  
ALEXANDRIA, VA 22333  
01CY ATTN DRCLDC J.A. BENDER

COMMANDER  
U.S. ARMY NUCLEAR AND CHEMICAL AGENCY  
7500 BACKLICK ROAD  
BLDG 2073  
SPRINGFIELD, VA 22150  
01CY ATTN LIBRARY

DIRECTOR  
U.S. ARMY BALLISTIC RESEARCH LABORATORY  
ABERDEEN PROVING GROUND, MD 21005  
01CY ATTN TECH LIBRARY EDWARD BAICY

COMMANDER  
U.S. ARMY SATCOM AGENCY  
FT. MONMOUTH, NJ 07703  
01CY ATTN DOCUMENT CONTROL

COMMANDER  
U.S. ARMY MISSILE INTELLIGENCE AGENCY  
REDSTONE ARSENAL, AL 35809  
01CY ATTN JIM GAMBLE

DIRECTOR  
U.S. ARMY TRADOC SYSTEMS ANALYSIS ACTIVITY  
WHITE SANDS MISSILE RANGE, NM 88002  
01CY ATTN ATAA-SA  
01CY ATTN TCC/F. PAYAN JR.  
01CY ATTN ATTA-TAC LTC J. HESSE

COMMANDER  
NAVAL ELECTRONIC SYSTEMS COMMAND  
WASHINGTON, D.C. 20360  
01CY ATTN NAVALEX 034 T. HUGHES  
01CY ATTN PME 117  
01CY ATTN PME 117-T  
01CY ATTN CODE 5011

COMMANDING OFFICER  
NAVAL INTELLIGENCE SUPPORT CTR  
4301 SUITLAND ROAD, BLDG. 5  
WASHINGTON, D.C. 20390  
01CY ATTN MR. DUBBIN STIC 12  
01CY ATTN NISC-50  
01CY ATTN CODE 5404 J. GALET

COMMANDER  
NAVAL OCCEAN SYSTEMS CENTER  
SAN DIEGO, CA 92152  
01CY ATTN J. FERGUSON

NAVAL RESEARCH LABORATORY  
WASHINGTON, D.C. 20375  
01CY ATTN CODE 4700 S. L. Ossakow  
26 CYS IF UNCLASS. 1 CY IF CLASS)  
01CY ATTN CODE 4701 I Vitkovitsky  
01CY ATTN CODE 4780 J. Huba (100  
CYS IF UNCLASS, 1 CY IF CLASS)  
01CY ATTN CODE 7500  
01CY ATTN CODE 7550  
01CY ATTN CODE 7580  
01CY ATTN CODE 7551  
01CY ATTN CODE 7555  
01CY ATTN CODE 4730 E. MCLEAN  
01CY ATTN CODE 4108  
01CY ATTN CODE 4730 B. RIPIN  
20CY ATTN CODE 2628

COMMANDER  
NAVAL SEA SYSTEMS COMMAND  
WASHINGTON, D.C. 20362  
01CY ATTN CAPT R. PITKIN

COMMANDER  
NAVAL SPACE SURVEILLANCE SYSTEM  
DAHLGREN, VA 22448  
01CY ATTN CAPT J.H. BURTON

OFFICER-IN-CHARGE  
NAVAL SURFACE WEAPONS CENTER  
WHITE OAK, SILVER SPRING, MD 20910  
01CY ATTN CODE F31

DIRECTOR  
STRATEGIC SYSTEMS PROJECT OFFICE  
DEPARTMENT OF THE NAVY  
WASHINGTON, D.C. 20376  
01CY ATTN NSP-2141  
01CY ATTN NSSP-2722 FRED WIMBERLY

COMMANDER  
NAVAL SURFACE WEAPONS CENTER  
DAHLGREN LABORATORY  
DAHLGREN, VA 22448  
01CY ATTN CODE DF-14 R. BUTLER

OFFICER OF NAVAL RESEARCH  
ARLINGTON, VA 22217  
01CY ATTN CODE 465  
01CY ATTN CODE 461  
01CY ATTN CODE 402  
01CY ATTN CODE 420  
01CY ATTN CODE 421

COMMANDER  
AEROSPACE DEFENSE COMMAND/DC  
DEPARTMENT OF THE AIR FORCE  
ENT AFB, CO 80912  
01CY ATTN DC MR. LONG

COMMANDER  
AEROSPACE DEFENSE COMMAND/XPD  
DEPARTMENT OF THE AIR FORCE  
ENT AFB, CO 80912  
01CY ATTN XPDQQ  
01CY ATTN XP

AIR FORCE GEOPHYSICS LABORATORY  
HANSOM AFB, MA 01731  
01CY ATTN OPR HAROLD GARDNER  
01CY ATTN LKB KENNETH S.W. CHAMPION  
01CY ATTN OPR ALVA T. STAIR  
01CY ATTN PHD JURGEN BUCHAU  
01CY ATTN PHD JOHN P. MULLEN

AF WEAPONS LABORATORY  
KIRTLAND AFT, NM 87117  
01CY ATTN SUL  
01CY ATTN CA ARTHUR H. GUENTHER  
01CY ATTN NYCE 1LT. G. KRAJEI

AFTAC  
PATRICK AFB, FL 32925  
01CY ATTN TF/MAJ WILEY  
01CY ATTN TN

AIR FORCE AVIONICS LABORATORY  
WRIGHT-PATTERSON AFB, OH 45433  
01CY ATTN AAD WADE HUNT  
01CY ATTN AAD ALLEN JOHNSON

DEPUTY CHIEF OF STAFF  
RESEARCH, DEVELOPMENT, & ACQ  
DEPARTMENT OF THE AIR FORCE  
WASHINGTON, D.C. 20330  
01CY ATTN AFRDQ

HEADQUARTERS  
ELECTRONIC SYSTEMS DIVISION  
DEPARTMENT OF THE AIR FORCE  
HANSOM AFB, MA 01731  
01CY ATTN J. DEAS

HEADQUARTERS  
ELECTRONIC SYSTEMS DIVISION/YSEA  
DEPARTMENT OF THE AIR FORCE  
HANSOM AFB, MA 01732  
01CY ATTN YSEA

HEADQUARTERS  
ELECTRONIC SYSTEMS DIVISION/DC  
DEPARTMENT OF THE AIR FORCE  
HANSOM AFB, MA 01731  
01CY ATTN DCKC MAJ J.C. CLARK

COMMANDER  
FOREIGN TECHNOLOGY DIVISION, AFSC  
WRIGHT-PATTERSON AFB, OH 45433  
01CY ATTN NICD LIBRARY  
01CY ATTN ETDP B. BALLARD

COMMANDER  
ROME AIR DEVELOPMENT CENTER, AFSC  
GRIFFISS AFB, NY 13441  
01CY ATTN DOC LIBRARY/TSLD  
01CY ATTN OCSE V. COYNE

SAMSO/SZ  
POST OFFICE BOX 92960  
WORLDWAY POSTAL CENTER  
LOS ANGELES, CA 90009  
(SPACE DEFENSE SYSTEMS)  
01CY ATTN SZJ

STRATEGIC AIR COMMAND/XPFS  
OFFUTT AFB, NB 68113  
01CY ATTN ADWATE MAJ BRUCE BAUER  
01CY ATTN NRT  
01CY ATTN DOK CHIEF SCIENTIST

SAMSO/SK  
P.O. BOX 92960  
WORLDWAY POSTAL CENTER  
LOS ANGELES, CA 90009  
01CY ATTN SKA (SPACE COMM SYSTEMS)  
M. CLAVIN

SAMSO/MN  
NORTON AFB, CA 92409  
(MINUTEMAN)  
01CY ATTN MNML

COMMANDER  
ROME AIR DEVELOPMENT CENTER, AFSC  
HANSOM AFB, MA 01731  
01CY ATTN EEP A. LORENTZEN

DEPARTMENT OF ENERGY  
LIBRARY ROOM G-042  
WASHINGTON, D.C. 20545  
01CY ATTN DOC CON FOR A. LABOWITZ

DEPARTMENT OF ENERGY  
ALBUQUERQUE OPERATIONS OFFICE  
P.O. BOX 5400  
ALBUQUERQUE, NM 87115  
01CY ATTN DOC CON FOR D. SHERWOOD

EG&G, INC.  
LOS ALAMOS DIVISION  
P.O. BOX 809  
LOS ALAMOS, NM 85544  
01CY ATTN DOC CON FOR J. BREEDLOVE

UNIVERSITY OF CALIFORNIA  
LAWRENCE LIVERMORE LABORATORY  
P.O. BOX 808  
LIVERMORE, CA 94550  
01CY ATTN DOC CON FOR TECH INFO DEPT  
01CY ATTN DOC CON FOR L-389 R. OTT  
01CY ATTN DOC CON FOR L-31 R. HAGER  
01CY ATTN DOC CON FOR L-46 F. SEWARD

LOS ALAMOS NATIONAL LABORATORY  
P.O. BOX 1663  
LOS ALAMOS, NM 87545  
01CY ATTN DOC CON FOR J. WOLCOTT  
01CY ATTN DOC CON FOR R.F. TASCHEK  
01CY ATTN DOC CON FOR E. JONES  
01CY ATTN DOC CON FOR J. MALIK  
01CY ATTN DOC CON FOR R. JEFFRIES  
01CY ATTN DOC CON FOR J. ZINN  
01CY ATTN DOC CON FOR P. KEATON  
01CY ATTN DOC CON FOR D. WESTERVELT  
01CY ATTN D. SAPPENFIELD

SANDIA LABORATORIES  
P.O. BOX 5800  
ALBUQUERQUE, NM 87115  
01CY ATTN DOC CON FOR W. BROWN  
01CY ATTN DOC CON FOR A. THORNBROUGH  
01CY ATTN DOC CON FOR T. WRIGHT  
01CY ATTN DOC CON FOR D. DAHLGREN  
01CY ATTN DOC CON FOR 3141  
01CY ATTN DOC CON FOR SPACE PROJECT DIV

SANDIA LABORATORIES  
LIVERMORE LABORATORY  
P.O. BOX 969  
LIVERMORE, CA 94550  
01CY ATTN DOC CON FOR B. MURPHAY  
01CY ATTN DOC CON FOR T. COOK

OFFICE OF MILITARY APPLICATION  
DEPARTMENT OF ENERGY  
WASHINGTON, D.C. 20545  
01CY ATTN DOC CON DR. YO SONG

OTHER GOVERNMENT

DEPARTMENT OF COMMERCE  
NATIONAL BUREAU OF STANDARDS  
WASHINGTON, D.C. 20234  
01CY (ALL CORRES: ATTN SEC OFFICER FOR)

INSTITUTE FOR TELECOM SCIENCES  
NATIONAL TELECOMMUNICATIONS & INFO ADMIN  
BOULDER, CO 80303  
01CY ATTN A. JEAN (UNCLASS ONLY)  
01CY ATTN W. UTLAUT  
01CY ATTN D. CROMBIE  
01CY ATTN L. BERRY

NATIONAL OCEANIC & ATMOSPHERIC ADMIN  
ENVIRONMENTAL RESEARCH LABORATORIES  
DEPARTMENT OF COMMERCE  
BOULDER, CO 80302  
01CY ATTN R. GRUBB  
01CY ATTN AERONOMY LAB G. REID

DEPARTMENT OF DEFENSE CONTRACTORS

AEROSPACE CORPORATION  
P.O. BOX 92957  
LOS ANGELES, CA 90009  
01CY ATTN I. GARFUNKEL  
01CY ATTN T. SALMI  
01CY ATTN V. JOSEPHSON  
01CY ATTN S. BOWER  
01CY ATTN D. OLSEN

ANALYTICAL SYSTEMS ENGINEERING CORP  
5 OLD CONCORD ROAD  
BURLINGTON, MA 01803  
01CY ATTN RADIO SCIENCES

AUSTIN RESEARCH ASSOC., INC.  
1901 RUTLAND DRIVE  
AUSTIN, TX 78758  
01CY ATTN L. SLOAN  
01CY ATTN R. THOMPSON

BERKELEY RESEARCH ASSOCIATES, INC.  
P.O. BOX 983  
BERKELEY, CA 94701  
01CY ATTN J. WORKMAN  
01CY ATTN C. PRETTIE  
01CY ATTN S. BRECHT

BOEING COMPANY, THE  
P.O. BOX 3707  
SEATTLE, WA 98124  
01CY ATTN G. KEISTER  
01CY ATTN D. MURRAY  
01CY ATTN G. HALL  
01CY ATTN J. KENNEY

CHARLES STARK DRAPER LABORATORY, INC.  
555 TECHNOLOGY SQUARE  
CAMBRIDGE, MA 02139  
01CY ATTN D.B. COX  
01CY ATTN J.P. GILMORE

COMSAT LABORATORIES  
LINTHICUM ROAD  
CLARKSBURG, MD 20734  
01CY ATTN G. HYDE

CORNELL UNIVERSITY  
DEPARTMENT OF ELECTRICAL ENGINEERING  
ITHACA, NY 14850  
01CY ATTN D.T. FARLEY, JR.

ELECTROSPACE SYSTEMS, INC.  
BOX 1359  
RICHARDSON, TX 75080  
01CY ATTN H. LOGSTON  
01CY ATTN SECURITY (PAUL PHILLIPS)

EOS TECHNOLOGIES, INC.  
606 Wilshire Blvd.  
Santa Monica, Calif 90401  
01CY ATTN C.B. GABBARD

ESL, INC.  
495 JAVA DRIVE  
SUNNYVALE, CA 94086  
01CY ATTN J. ROBERTS  
01CY ATTN JAMES MARSHALL

GENERAL ELECTRIC COMPANY  
SPACE DIVISION  
VALLEY FORGE SPACE CENTER  
GODDARD BLVD KING OF PRUSSIA  
P.O. BOX 8555  
PHILADELPHIA, PA 19101  
01CY ATTN M.H. BORTNER SPACE SCI LAB

GENERAL ELECTRIC COMPANY  
P.O. BOX 1122  
SYRACUSE, NY 13201  
01CY ATTN F. REIBERT

GENERAL ELECTRIC TECH SERVICES CO., INC.  
RMES  
COURT STREET  
SYRACUSE, NY 13201  
01CY ATTN G. MILLMAN

GEOPHYSICAL INSTITUTE  
UNIVERSITY OF ALASKA  
FAIRBANKS, AK 99701  
(ALL CLASS ATTN: SECURITY OFFICER)  
01CY ATTN T.N. DAVIS (UNCLASS ONLY)  
01CY ATTN TECHNICAL LIBRARY  
01CY ATTN NEAL BROWN (UNCLASS ONLY)

GTE SYLVANIA, INC.  
ELECTRONICS SYSTEMS GRP-EASTERN DIV  
77 A STREET  
NEEDHAM, MA 02194  
01CY ATTN DICK STEINHOF

HSS, INC.  
2 ALFRED CIRCLE  
BEDFORD, MA 01730  
01CY ATTN DONALD HANSEN

ILLINOIS, UNIVERSITY OF  
107 COBLE HALL  
150 DAVENPORT HOUSE  
CHAMPAIGN, IL 61820  
(ALL CORRES ATTN DAN MCCLELLAND)  
01CY ATTN K. YEH

INSTITUTE FOR DEFENSE ANALYSES  
1801 NO. BEAUREGARD STREET  
ALEXANDRIA, VA 22311  
01CY ATTN J.M. AEIN  
01CY ATTN ERNEST BAUER  
01CY ATTN HANS WOLFARD  
01CY ATTN JOEL BENGSTON

INTL TEL & TELEGRAPH CORPORATION  
500 WASHINGTON AVENUE  
NUTLEY, NJ 07110  
01CY ATTN TECHNICAL LIBRARY

JAYCOR  
11011 TORREYANA ROAD  
P.O. BOX 85154  
SAN DIEGO, CA 92138  
01CY ATTN J.L. SPERLING

JOHNS HOPKINS UNIVERSITY  
APPLIED PHYSICS LABORATORY  
JOHNS HOPKINS ROAD  
LAUREL, MD 20810  
01CY ATTN DOCUMENT LIBRARIAN  
01CY ATTN THOMAS POTEMRA  
01CY ATTN JOHN DASSOULAS

KAMAN SCIENCES CORP  
P.O. BOX 7463  
COLORADO SPRINGS, CO 80933  
01CY ATTN T. MEAGHER

KAMAN TEMPO-CENTER FOR ADVANCED STUDIES  
816 STATE STREET (P.O DRAWER QQ)  
SANTA BARBARA, CA 93102  
01CY ATTN DASLAC  
01CY ATTN WARREN S. KNAPP  
01CY ATTN WILLIAM McNAMARA  
01CY ATTN B. GAMBILL

LINKABIT CORP  
10453 ROSELLE  
SAN DIEGO, CA 92121  
01CY ATTN IRWIN JACOBS

LOCKHEED MISSILES & SPACE CO., INC  
P.O. BOX 504  
SUNNYVALE, CA 94088  
01CY ATTN DEPT 60-12  
01CY ATTN D.R. CHURCHILL

LOCKHEED MISSILES & SPACE CO., INC.  
3251 RANOVER STREET  
PALO ALTO, CA 94304  
01CY ATTN MARTIN WALT DEPT 52-12  
01CY ATTN W.L. IMHOFF DEPT 52-12  
01CY ATTN RICHARD G. JOHNSON DEPT 52-12  
01CY ATTN J.B. CLADIS DEPT 52-12

MARTIN MARIETTA CORP  
ORLANDO DIVISION  
P.O. BOX 5837  
ORLANDO, FL 32805  
01CY ATTN R. HEFFNER

M.I.T. LINCOLN LABORATORY  
P.O. BOX 73  
LEXINGTON, MA 02173  
01CY ATTN DAVID M. TOWLE  
01CY ATTN L. LOUGHLIN  
01CY ATTN D. CLARK

MCDONNELL DOUGLAS CORPORATION  
5301 BOLSA AVENUE  
HUNTINGTON BEACH, CA 92647  
01CY ATTN N. HARRIS  
01CY ATTN J. MOULE  
01CY ATTN GEORGE MROZ  
01CY ATTN W. OLSON  
01CY ATTN R.W. HALPRIN  
01CY ATTN TECHNICAL LIBRARY SERVICES

MISSION RESEARCH CORPORATION  
735 STATE STREET  
SANTA BARBARA, CA 93101  
01CY ATTN P. FISCHER  
01CY ATTN W.F. CREVIER  
01CY ATTN STEVEN L. GUTSCHE  
01CY ATTN R. BOGUSCH  
01CY ATTN R. HENDRICK  
01CY ATTN RALPH KILB  
01CY ATTN DAVE SOWLE  
01CY ATTN F. FAJEN  
01CY ATTN M. SCHEIBE  
01CY ATTN CONRAD L. LONGMIRE  
01CY ATTN B. WHITE

MISSION RESEARCH CORP.  
1720 RANDOLPH ROAD, S.E.  
ALBUQUERQUE, NEW MEXICO 87106  
01CY R. STELLINGWERF  
01CY M. ALME  
01CY L. WRIGHT

MITRE CORPORATION, THE  
P.O. BOX 208  
BEDFORD, MA 01730  
01CY ATTN JOHN MORGANSTERN  
01CY ATTN G. HARDING  
01CY ATTN C.E. CALLAHAN

MITRE CORP  
WESTGATE RESEARCH PARK  
1820 DOLLY MADISON BLVD  
MCLEAN, VA 22101  
01CY ATTN W. HALL  
01CY ATTN W. FOSTER

PACIFIC-SIERRA RESEARCH CORP  
12340 SANTA MONICA BLVD.  
LOS ANGELES, CA 90025  
01CY ATTN E.C. FIELD, JR.

PENNSYLVANIA STATE UNIVERSITY  
IONOSPHERE RESEARCH LAB  
318 ELECTRICAL ENGINEERING EAST  
UNIVERSITY PARK, PA 16802  
(NO CLASS TO THIS ADDRESS)  
01CY ATTN IONOSPHERIC RESEARCH LAB

PHOTOMETRICS, INC.  
4 ARROW DRIVE  
WOBBURN, MA 01801  
01CY ATTN IRVING L. KOFSKY

PHYSICAL DYNAMICS, INC.  
P.O. BOX 3027  
BELLEVUE, WA 98009  
01CY ATTN E.J. FREMOUW

PHYSICAL DYNAMICS, INC.  
P.O. BOX 10367  
OAKLAND, CA 94610  
ATTN A. THOMSON

R & D ASSOCIATES  
P.O. BOX 9695  
MARINA DEL REY, CA 90291  
01CY ATTN FORREST GILMORE  
01CY ATTN WILLIAM B. WRIGHT, JR.  
01CY ATTN ROBERT F. LELEVIER  
01CY ATTN WILLIAM J. KARZAS  
01CY ATTN H. ORY  
01CY ATTN C. MACDONALD  
01CY ATTN R. TURCO  
01CY ATTN L. DERAND  
01CY ATTN W. TSAI

RAND CORPORATION, THE  
1700 MAIN STREET  
SANTA MONICA, CA 90406  
01CY ATTN CULLEN CRAIN  
01CY ATTN ED BEDROZIAN

RAYTHEON CO.  
528 BOSTON POST ROAD  
SUDBURY, MA 01776  
01CY ATTN BARBARA ADAMS

RIVERSIDE RESEARCH INSTITUTE  
330 WEST 42nd STREET  
NEW YORK, NY 10036  
01CY ATTN VINCE TRAPANI

SCIENCE APPLICATIONS, INC.  
1150 PROSPECT PLAZA  
LA JOLLA, CA 92037  
O1CY ATTN LEWIS M. LINSON  
O1CY ATTN DANIEL A. HAMLIN  
O1CY ATTN E. FRIEMAN  
O1CY ATTN E.A. STRAKER  
O1CY ATTN CURTIS A. SMITH  
O1CY ATTN JACK McDougall

SCIENCE APPLICATIONS, INC  
1710 GOODRIDGE DR.  
MCLEAN, VA 22102  
ATTN: J. COCKAYNE

SRI INTERNATIONAL  
333 RAVENSWOOD AVENUE  
MENLO PARK, CA 94025  
O1CY ATTN DONALD NEILSON  
O1CY ATTN ALAN BURNS  
O1CY ATTN G. SMITH  
O1CY ATTN R. TSUNODA  
O1CY ATTN DAVID A. JOHNSON  
O1CY ATTN WALTER G. CHESNUT  
O1CY ATTN CHARLES L. RINO  
O1CY ATTN WALTER JAYE  
O1CY ATTN J. VICKREY  
O1CY ATTN RAY L. LEADABRAND  
O1CY ATTN G. CARPENTER  
O1CY ATTN G. PRICE  
O1CY ATTN R. LIVINGSTON  
O1CY ATTN V. GONZALES  
O1CY ATTN D. MCDANIEL

TECHNOLOGY INTERNATIONAL CORP  
75 WIGGINS AVENUE  
BEDFORD, MA 01730  
O1CY ATTN W.P. BOQUIST

TOYON RESEARCH CO.  
P.O. Box 6890  
SANTA BARBARA, CA 93111  
O1CY ATTN JOHN ISE, JR.  
O1CY ATTN JOEL GARBARINO

TRW DEFENSE & SPACE SYS GROUP  
ONE SPACE PARK  
REDONDO BEACH, CA 90278  
O1CY ATTN R. K. PLEBUCH  
O1CY ATTN S. ALTSCHULER  
O1CY ATTN D. DEE  
O1CY ATTN D/ STOCKWELL  
SNTF/1575

VISIDYNE  
SOUTH BEDFORD STREET  
BURLINGTON, MASS 01803  
O1CY ATTN W. REIDY  
O1CY ATTN J. CARPENTER  
O1CY ATTN C. HUMPHREY

